doi:10.1038/nature16154

Contents

Experimental Details

General Considerations

Unless otherwise specified, all operations were carried out in an MBraun drybox under a nitrogen atmosphere or using standard Schlenk and vacuum line techniques. Pre-reduced Teflon-coated stir bars (prepared via stirring a Na[$C_{10}H_8$] solution overnight followed by rinsing three times with THF) were utilized in any stirred reaction in which KC_8, K[$C_{10}H_8$], **3**, or **4** were employed as reagents. Solvents for air- and moisture-sensitive reactions were dried over sodium benzophenone ketyl, calcium hydride, or by the method of Grubbs.[1] Deuterated solvents were purchased from Cambridge Isotope Laboratories and vacuum transferred from sodium benzophenone ketyl (C_6D_6, THF-d_8) or used without further purification ($CDCl_3$). Solvents, once dried and degassed, were vacuum transferred directly prior to use or stored under inert atmosphere over 4 Å molecular sieves. Dicarbonyl dication **1**,[2] $P_2Mo(MeCN)_2^{2OTf}$,[2] potassium graphite (KC_8),[3] (*Z*)-((2-bromovinyl)oxy)triisopropylsilane,[4] and tetrabutylammonium fluoride ($^nBu_4NF$)[5] were prepared and purified according to literature procedures. K[$C_{10}H_8$] was prepared by stirring a THF solution of naphthalene in a 20 mL scintillation vial charged with a K^0 mirror and a pre-reduced Teflon-coated stir bar for a minimum of two hours prior to use. Unless indicated otherwise, all other chemicals were utilized as received. Silver trifluoromethanesulfonate (triflate, OTf), graphite (325 mesh), *n*-butyl lithium (2.5 M in hexanes), and trimethylsilyl chloride (dried over CaH_2 and distilled prior to use) were purchased from Alfa Aesar. Sodium tetraphenyl borate (dried under vacuum at 50 °C, 12h), naphthalene (sublimed under reduced pressure at 40 °C), potassium metal, diisopropyl amine (dried over CaH_2 and distilled prior to use), hexafluorobenzene (dried over CaH_2 and distilled prior to use), and tetrabutlyammonium cyanide (dried under vacuum at 40 °C, 12h) were all purchased from Sigma Aldrich. ^{13}CO gas was purchased from Monsanto Research. Triisopropylsilyl chloride (dried over CaH_2 and distilled prior to use) was purchased from Oakwood Chemicals. ^1H, $^{13}C\{^1H\}$, and $^{31}P\{^1H\}$ NMR spectra were recorded on Varian Mercury 300 MHz, Varian 400 MHz, Bruker Ascend 400 MHz (equipped with a Prodigy Cryoprobe), or Varian INOVA-500 spectrometers with shifts reported in parts per million (ppm). ^1H and $^{13}C\{^1H\}$ NMR spectra are referenced to residual solvent peaks.[6] $^{31}P\{^1H\}$ chemical shifts are referenced to an external 85% H_3PO_4 (0 ppm) standard. Multiplicities and their descriptions are abbreviated as follows: s = singlet, d = doublet, dd = doublet of doublets, t = triplet, vt = virtual triplet, sext = sextet, sept d = septet of doublets, m = multiplet, and br = broad. Fourier transform infrared ATR spectra were collected from thin films or powders on a Thermo Scientific Nicolet iS5 Spectrometer with a diamond ATR crystal (utilized iD5 ATR insert). Elemental analysis was conducted by Robertson Microlit Laboratories, Inc. (Ledgewood, NJ) or Midwest Microlabs, LLC (Indianapolis, IN).

Synthesis of 2

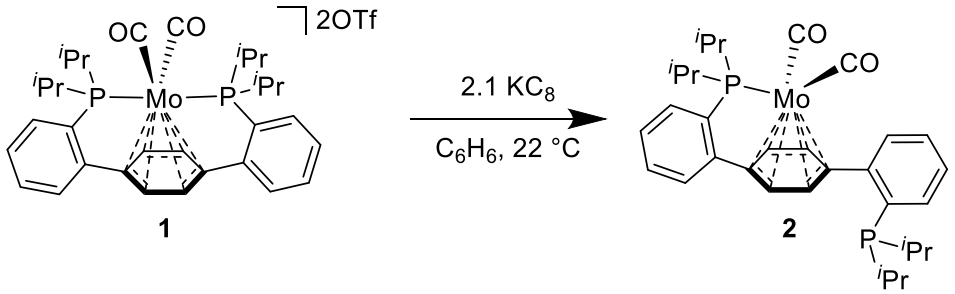

To a vigorously stirring suspension of **1** (200 mg, 0.217 mmol) in C_6H_6 (10 mL), solid KC_8 (62 mg, 0.456 mmol) was added in a single portion, resulting in an immediate darkening of the mixture. Stirring continued for 30 minutes at which time the solution as filtered through a Celite plug. The deep yellow filtrate was lyophilized, providing **2** as a yellow powder (120 mg, 0.195 mmol, 90%). Diffusion of pentane into a saturated C_6H_6 solution of **2** provided single crystals suitable for X-ray diffraction. ^1H

NMR (400 MHz, C_6D_6, 25 °C) δ: 7.98-8.03 (m, 1H, aryl-*H*), 7.24-7.29 (m, 1H, aryl-*H*), 7.01-7.07 (m, 2H, aryl-*H*), 6.86-6.96 (m, 4H, aryl-*H*), 5.41 (d, *J* = 5.66 Hz, 2H, central arene-*H*), 4.52 (dd, *J* = 6.11, 1.87 Hz, 2H, central arene-*H*), 2.18-2.30 (m, 2H, C*H*$(CH_3)_2$), 1.83-1.94 (sept d, *J* = 6.97, 1.90 Hz, 2H, C*H*$(CH_3)_2$), 1.18 (dd, *J* = 16.54, 6.84 Hz, 6H, CH(C*H*$_3)_2$), 1.03 (dd, *J* = 14.87, 7.05 Hz, 6H, CH(C*H*$_3)_2$), 0.91 (dd, *J* = 8.73, 6.98 Hz, 6H, CH(C*H*$_3)_2$), 0.87 (t, *J* = 7.19 Hz, 6 H, CH(C*H*$_3)_2$). $^{13}C\{^1H\}$ NMR (101 MHz, C_6D_6, 25 °C) δ: 228.5 (d, *J* = 11.63 Hz, *C*O), 147.11 (d, *J* = 27.80 Hz, aryl-*C*), 146.60 (d, *J* = 21.84 Hz, aryl-*C*), 145.89 (d, *J* = 27.80 Hz, aryl-*C*), 136.21 (d, *J* = 21.64 Hz, aryl-*C*), 135.97 (d, *J* = 4.73 Hz, aryl-*C*), 131.78 (d, *J* = 3.44 Hz, aryl-*C*), 129.37 (d, *J* = 1.06 Hz, aryl-*C*), 129.34 (d, *J* = 2.13 Hz, aryl-*C*), 129.20 (s, aryl-*C*), 127.47 (s, aryl-*C*), 127.34 (s, aryl-*C*), 127.23 (s, aryl-*C*), 123.54 (d, *J* = 3.54 Hz, central arene-*C*), 108.53 (dd, *J* = 9.33, 3.35 Hz, central arene-*C*), 92.30 (dd, *J* = 5.52, 1.35 Hz, central arene-*C*), 82.34 (d, *J* = 2.21 Hz, central arene-*C*), 28.57 (d, *J* = 21.46, *C*H$(CH_3)_2$), 25.27 (d, *J* = 14.89, *C*H$(CH_3)_2$), 20.71 (d, *J* = 19.85, CH(*C*H$_3)_2$), 19.97 (d, *J* = 10.94, CH(*C*H$_3)_2$), 18.97 (d, *J* = 6.06, CH(*C*H$_3)_2$), 18.87 (d, *J* = 0.99, CH(*C*H$_3)_2$). $^{31}P\{^1H\}$ NMR (162 MHz, C_6D_6, 25 °C) δ: 92.33 (s, Mo-*P*), -7.32 (s). IR (THF cast thin film, cm^{-1}) ν_{CO}: 1887, 1832. Anal. Calcd. for **2** $C_{32}H_{40}MoO_2P_2$ (%): C, 62.54; H, 6.56; N, 0.00 Found: C, 62.75; H, 6.68; N, <0.02.

2-^{13}CO was prepared analogously starting from **1-^{13}CO**; the enhanced resonance in the $^{13}C\{^1H\}$ NMR spectrum is the doublet at 228.5 ppm and the $^{31}P\{^1H\}$ NMR signal at 92.33 ppm is split into a triplet (*J* = 11.46 Hz). IR (THF cast thin film, cm^{-1}) ν_{13CO}: 1847, 1793.

Synthesis of **3**

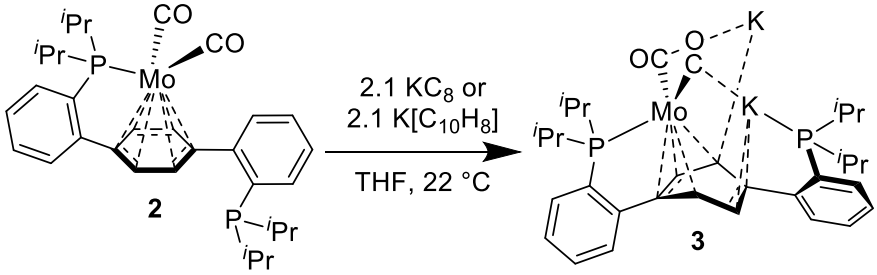

Method A (KC_8): To a stirring yellow solution of **2** (200 mg, 0.325 mmol) in THF (10 mL), KC_8 (92.3 mg, 0.683 mmol) was added as a solid in a single portion, resulting in an immediate color change to dark red. Stirring continued for 10 minutes, at which time the mixture was filtered through a Celite plug. The burgundy filtrate was dried *in vacuo*, providing a tacky residue. Trituration with hexanes and removal of the volatiles under reduced pressure gave **3** as a red powder (262 mg, 0.288 mmol, 89%—NB: values were calculated using the molecular weight for **3•THF$_3$**, $C_{44}H_{64}K_2MoO_5P_2$, 909.10 g/mol). X-ray quality crystals of **3** were obtained via chilling a saturated THF/pentane (3:1) mixture of **3** (-35 °C).

Method B ($K[C_{10}H_8]$): To a stirring yellow solution of **2** (200 mg, 0.325 mmol) in THF (7 mL), a deep green $K[C_{10}H_8]$ (0.683 mmol) solution in THF (3 mL) was added dropwise. With added reductant, the yellow color gave way to a persistent deep red. Following complete addition, stirring continued for 45 minutes, at which time volatiles were removed *in vacuo*. The resulting red residue was triturated with hexanes and dried. Addition of hexanes suspended the red solids, which were collected on a fritted funnel. Washing of the filter cake with a mixture of hexanes and benzene (1:1) and collection of the solids provided **3** as a red powder (211 mg, 0.232 mmol, 71%—NB: values were calculated using the molecular weight for **3•THF$_3$**, $C_{44}H_{64}K_2MoO_5P_2$, 909.10 g/mol).

Due to the extreme air and moisture sensitivity of **3**, its preparation is recommended in small batches. All samples of **3** were stored in the solid state at -35 °C.

^{1}H NMR (400 MHz, THF-d_8, 25 °C) δ: 7.17 (br s, 2H, aryl-*H*), 7.04 (br s, 2H, aryl-*H*), 6.86-6.93 (br m, 2H, aryl-*H*), 6.64 (br s, 1H, aryl-*H*), 6.36 (br s, 1H, central arene-*H*), 5.62-5.70 (br m, 2H, central arene-*H*), 5.31 (br s, 1H, central arene-*H*), 2.14 (br m, 4H, C*H*(CH_3)$_2$), 0.74-1.19 (br m, 24H, CH(CH_3)$_2$). ^{31}P{^{1}H} NMR (162 MHz, THF-d_8, 25 °C) δ: 104.62 (s, Mo-P), 102.47 (br s, Mo-P), -0.03 (s), -2.66 (s). IR (powder sample, diamond ATR, cm^{-1}) ν_{CO}: 1657, 1570. The broad NMR and IR spectra of **3** are attributed to fluxionality between oligomeric forms in solution. Anal. Calcd. for **3** $C_{32}H_{40}K_2MoO_2P_2$ (%): C, 55.48; H, 5.82; N, 0.00. Found: C, 54.38; H, 6.03; N, <0.02. Duplicate samples analyzed at different laboratories failed to provide satisfactory combustion analysis results, likely due to the presence of residual oxygen (≥20 ppm) in the gloveboxes at these facilities.

3-^{13}CO was prepared analogously starting from **2-^{13}CO**; the isotopically enhanced carbonyl carbons resonated as broad signals at 263.80 and 245.67 ppm and at 265.87, 260.90, 246.04, and 243.85 ppm in the 25 °C ^{13}C{^{1}H} and -80 °C ^{13}C{^{1}H} NMR spectra, respectively. IR (powder sample, diamond ATR, cm^{-1}) ν_{13CO}: 1621, 1534.

Synthesis of **4**

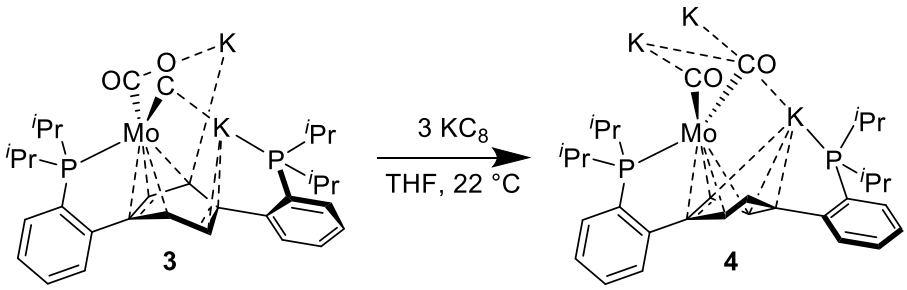

3 **4**

To a stirring red solution of **3** (107 mg, 0.117 mmol) in THF (6 mL), KC_8 (48 mg, 0.351 mmol) was added as a solid in a single portion, resulting in an immediate color change to deep purple. Stirring continued for 30 minutes, at which time the mixture was filtered through a Celite plug. The filtrate was concentrated *in vacuo* to *ca.* 1 mL, layered with pentane (10 mL), and chilled (-35 °C) for 16 hours. Filtration, collection of the solids, and removal of residual volatiles under reduced pressure provided **4** as purple microcrystals (98 mg, 0.107 mmol, 92%—NB: values were calculated using the molecular weight for **4•THF$_{2.5}$**, $C_{42}H_{60}K_3MoO_{4.5}P_2$, 912.14 g/mol). Single crystals of **4** suitable for X-ray diffraction were obtained via chilling a saturated THF/pentane (3:1) mixture (-35 °C).

Due to the extreme air and moisture sensitivity of **4**, its preparation is recommended in small batches. All samples of **4** were stored in the solid state at -35 °C.

Anal. Calcd. for **4•THF$_{2.5}$** $C_{42}H_{60}K_3MoO_{4.5}P_2$ (%): C, 55.31; H, 6.63; N, 0.00. Found: C, 54.33; H, 6.24; N, <0.02. These CHN combustion analysis results are in agreement with those expected for **4•THF$_{1.5}$**: C, 54.40; H, 6.13; N, 0.00.

4-^{13}CO was prepared analogously starting from **3-^{13}CO**.

Synthesis of **6a**

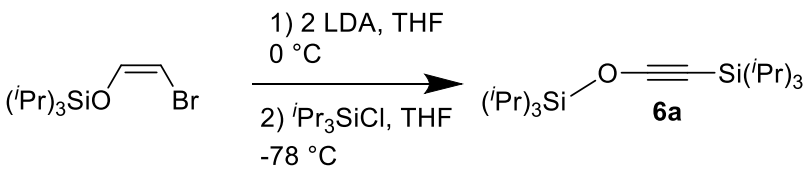

6a

6a was prepared via a modified literature procedure for the synthesis of trialkylsilyloxyethyne derivatives.[4] An oven-dried Schlenk flask, charged with a stir bar, was cooled to ambient temperature under vacuum. The flask was backfilled with argon before THF (50 mL) and freshly distilled diisopropyl amine (1.05 mL, 7.49 mmol) were added via cannula and syringe, respectively. The reaction vessel was cooled to 0 °C with stirring and ^{n}BuLi (3 mL, 2.5 M in hexanes, 7.50 mmol) was added via syringe. After stirring for 15 minutes, a solution of (*Z*)-(2-bromovinyl)triisopropylsilane (1.00 g, 3.58 mmol) in THF (10 mL) was added via cannula. Stirring at 0 °C continued for 75 minutes. At this time, the flask was cooled to -78 °C and ^{i}Pr$_3$SiCl (1.5 mL, 7.01 mmol) was added via syringe. Stirring continued for 10 minutes at -78 °C at which point the flask was removed from the bath and allowed to warm to room temperature. Volatiles were removed under reduced pressure, providing a mixture of off-white solids and a yellow oil. This mixture was separated via Kugelrohr distillation (85 °C, 0.01 mm Hg), giving **6a** as a colorless oil (685 mg, 1.93 mmol, 54%). ^{1}H NMR (500 MHz, $CDCl_3$, 25 °C) δ: 1.30 (sext, *J* = 7.42 Hz, 1H, C*H*(CH$_3$)$_3$), 1.14 (d, *J* = 7.42 Hz, 6H, CH(C*H*$_3$)$_3$), 1.04 (d, *J* = 6.91 Hz, 6H, CH(C*H*$_3$)$_3$), 0.98 (sext, *J* = 6.91 Hz, 1H, C*H*(CH$_3$)$_3$). ^{13}C{^{1}H} NMR (126 MHz, C_6D_6, 25 °C) δ: 108.27 (s, O*C*CSi), 25.18 (s, OC*C*Si), 18.86 (br s, *C*H(CH$_3$)$_3$), 17.46 (br s, *C*H(CH$_3$)$_3$), 12.02 (s, CH(*C*H$_3$)$_3$), 11.92 (s, CH(*C*H$_3$)$_3$).

Synthesis of **7**

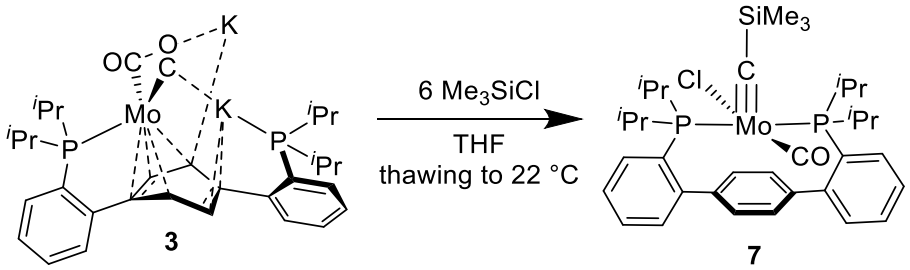

A 20 mL scintillation vial was charged with **3** (200 mg, 0.220 mmol), THF (7 mL), and a stir bar. The resulting deep red solution was frozen in a liquid nitrogen-cooled cold well. A second 20 mL scintillation vial was charged with a Me_3SiCl (188 mg, 1.73 mmol) solution in THF (3 mL) and likewise frozen. Immediately upon thawing, the Me_3SiCl solution was added dropwise to a thawing and stirring solution of **3**. Stirring at room temperature continued for 20 minutes, during which time the solution lightened to a red/orange. At this time, volatiles were removed *in vacuo*. The resulting red residue was triturated with 2 mL of hexanes and dried under reduced pressure, providing **7** as a deep red powder (121 mg, 0.172 mmol, 78%). In all instances, **7** prepared this way contained *ca.* 5% **2** as observed by ^{1}H and ^{31}P{^{1}H} NMR. Separation was achieved by first washing with cold HMDSO (3 x 2 mL) and then washing with C_6H_6 (1 mL). Dissolving the remaining solids in C_6H_6 (5 mL) and lyophilizing provided analytically pure **7** as a red powder (44 mg, 0.063 mmol, 29%). X-ray quality crystals were obtained from vapor diffusion of pentane into a saturated C_6H_6 solution of **7**. ^{1}H NMR (400 MHz, C_6D_6, 25 °C) δ: 7.48-7.51 (m, 2H, aryl-*H*), 7.45 (m, 2H, central arene-*H*), 7.32-7.34 (m, 2H, central arene-*H*), 7.28-7.31 (m, 2H, aryl-*H*), 7.16 (t, *J* = 7.90 Hz, 2H, aryl-*H*), 7.12 (dt, *J* = 7.27, 1.71 Hz, 2H, aryl-*H*), 2.63-2.80 (m, 4H, C*H*(CH$_3$)$_2$), 2.02-2.08 (m, 6H, CH(C*H*$_3$)$_2$), 1.77-1.82 (m, 6H, CH(C*H*$_3$)$_2$), 1.04-1.08 (m, 6H, CH(C*H*$_3$)$_2$), 0.86-0.91 (m, 6 H, CH(C*H*$_3$)$_2$), 0.11 (s, 9H, Si(C*H*$_3$)$_3$). ^{13}C{^{1}H} NMR (101 MHz, C_6D_6, 25 °C) δ: 355.69-356.02 (m, *C*SiMe$_3$), 247.27-247.56 (m, *C*O), 148.18 (vt, *J* = 6.85 Hz, aryl-*C*), 140.32 (vt, *J* = 2.64 Hz, aryl-*C*), 132.61 (s, aryl-*C*), 132.32 (vt, *J* = 9.96 Hz, aryl-*C*), 130.17 (s, aryl-*C*), 129.59 (vt, *J* = 2.54 Hz, aryl-*C*), 129.55 (s, aryl-*C*), 127.30 (vt, *J* = 2.50 Hz, aryl-*C*), 125.07 (vt, *J* = 2.47, aryl-*C*), 36.92 (vt, *J* = 8.36, *C*H(CH$_3$)$_2$), 27.74 (vt, *J* = 27.74, *C*H(CH$_3$)$_2$), 20.19 (s, CH(*C*H$_3$)$_2$), 19.82 (s, CH(*C*H$_3$)$_2$), 19.77 (vt, *J* = 5.71, *C*H(CH$_3$)$_2$), 18.49 (vt, *J* = 3.49, *C*H(CH$_3$)$_2$), 0.11 (s, Si(*C*H$_3$)$_3$). ^{31}P{^{1}H} NMR (162 MHz, C_6D_6, 25 °C) δ: 36.63 (s). IR (THF cast thin film, cm^{-1}) ν_{CO}: 1873. Anal. Calcd. for **7** $C_{35}H_{49}ClMoOP_2Si$ (%): C, 59.44; H, 6.98; N, 0.00 Found: C, 59.16; H, 6.77; N, <0.02.

7-^{13}CO was prepared analogously starting from **3-^{13}CO**; the enhanced resonances in the $^{13}C\{^1H\}$ NMR spectrum are the multiplets at 355.85 ppm (J_{PC} = 13.25 Hz, J_{CC} = 8.9 Hz) and 247.42 (J_{PC} = 11.35 Hz, J_{CC} = 8.9 Hz) ppm. The $^{31}P\{^1H\}$ NMR signal at 36.63 ppm is split into a doublet of doublets (J = 13.25, 11.35 Hz).

Synthesis of **8-^{13}CO**

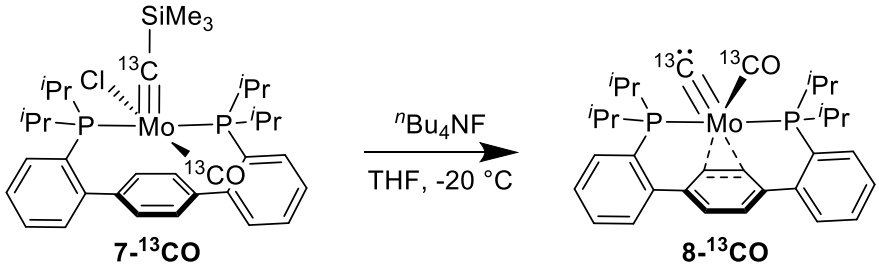

7-^{13}CO **8-^{13}CO**

Due to thermal instability, **8-^{13}CO** must be prepared *in situ*. In a typical procedure, a J. Young NMR tube was charged with **7-^{13}CO** (20 mg, 0.028 mmol) and ^{n}Bu$_4$NF (7.3 mg, 0.028 mmol). The headspace of the NMR tube was evacuated and THF-d_8 (0.4 mL) admitted at -196 °C via vacuum transfer. The contents of the J. Young tube were thawed to -80 °C and mixed. Warming to -20 °C in the NMR probe for 15 minutes showed complete conversion to **8-^{13}CO** by $^{13}C\{^1H\}$ and $^{31}P\{^1H\}$ NMR spectroscopy and solutions prepared this way were re-cooled to -80 °C and used without further manipulation. THF solutions of **8-^{13}CO** were stable at -80 °C, but demonstrated decomposition to intractable mixtures when allowed to warm to temperatures exceeding 0 °C. ^{1}H NMR (500 MHz, THF-d_8, -20 °C) δ: 7.96 (br s, 2H, aryl-*H*), 7.57 (d, J = 3.57 Hz, 2H, aryl-*H*), 7.56 (d, J = 3.57 Hz, 2H, aryl-*H*), 7.43 (br s, 2H, aryl-*H*), 6.71 (s, 2H, central arene-*H*), 6.46 (br t, J = 2.20 Hz, 2H, central arene-*H*), 3.13-3.21 (m, 2H, C*H*(CH$_3$)$_2$), 2.45-2.53 (m, 2H, C*H*(CH$_3$)$_2$), 1.64-1.68 (m, 6H, CH(C*H*$_3$)$_2$), 1.55-1.59 (m, 2H, CH(C*H*$_3$)$_2$), 1.02-1.05 (m, 6H, CH(C*H*$_3$)$_2$), 0.21-026 (m, 6H, CH(C*H*$_3$)$_2$). $^{13}C\{^1H\}$ NMR (126 MHz, THF-d_8, -80 °C) δ: 546.20 (br s, *C:*), 233.16 (t, J = 12.25 Hz, *C*O), 150.72 (vt, J = 7.13 Hz, aryl-*C*), 139.73 (vt, J = 3.85 Hz, aryl-*C*), 132.69 (vt, J = 4.23 Hz, aryl-*C*), 130.98 (br s, aryl-*C*), 129.18 (br s, aryl-*C*), 128.49 (br s, aryl-*C*), 128.28 (br s, aryl-*C*), 124.00 (vt, J = 8.63 Hz, central arene-*C*), 86.17 (s, central arene-*C*), 29.97 (vt, J = 8.63 Hz, *C*H(CH$_3$)$_2$), 23.53 (br s, *C*H(CH$_3$)$_2$), 20.11 (br s, CH(*C*H$_3$)$_2$), 17.20 (br s, CH(*C*H$_3$)$_2$), 16.77 (br s, CH(*C*H$_3$)$_2$). $^{31}P\{^1H\}$ NMR (202 MHz, THF-d_8, -80 °C) δ: 51.66 (d, J = 12.55 Hz). NMR spectra collected at 25 °C demonstrated resolved C–C and P–C coupling, despite decomposition over the course of the experiments, splitting the resonances as follows: $^{13}C\{^1H\}$ NMR (126 MHz, THF/C_6D_6, 25 °C) δ: 546.20 (dd, J = 3.46, 3.26 Hz, *C:*), 233.16 (dd, J = 12.55, 3.46 Hz, *C*O). $^{31}P\{^1H\}$ NMR (202 MHz, THF/C_6D_6, 25 °C) δ: 51.66 (dd, J = 12.55, 3.26 Hz).

Synthesis of **1-^{13}CO**

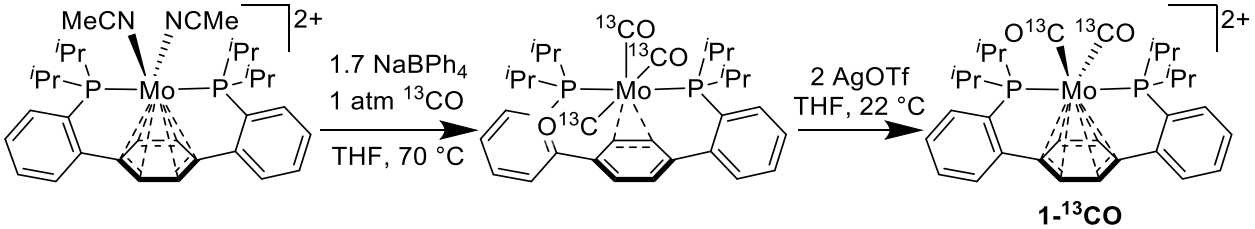

1-^{13}CO

To a 500 mL Schlenk tube charged with a stir bar, P$_2$Mo(MeCN)$_2^{2OTf}$ (2.3 g, 2.45 mmol), and NaBPh$_4$ (1.4 g, 4.09 mmol), THF (120 mL) was added via cannula. Stirring was initiated, providing a purple/green heterogeneous mixture. The contents of the Schlenk were freeze-pump-thawed thrice, and ^{13}CO (1 atm, *ca.* 14.3 mmol) was admitted to the reaction vessel. The Schlenk was sealed, heated to 70 °C, and stirred for 48 hours, resulting in the formation of a deep orange homogeneous solution. Volatiles were removed

in vacuo, giving an orange residue. Addition of pentane (100 mL) via cannula, sonication, and filtration provided $P_2Mo(^{13}CO)_3$ as an orange powder (1.35 g, 2.1 mmol, 86%). Spectral features of $P_2Mo(^{13}CO)_3$ match those reported for $P_2Mo(CO)_3$,[2] except the triplets in the $^{13}C\{^1H\}$ NMR at 221.15 and 213.75 ppm are enhanced and the $^{31}P\{^1H\}$ NMR resonance at 51.01 ppm is split into a quartet (J = 9.33 Hz).

From $P_2Mo(^{13}CO)_3$, **1-^{13}CO** can be prepared via the procedure reported for the ^{12}CO isotopolog in comparable yield.[2] Spectral features of **1-^{13}CO** match those of **1**, except the $^{13}C\{^1H\}$ resonance at 219.03 ppm is enhanced, the $^{31}P\{^1H\}$ NMR resonance at 75.05 ppm is split into a triplet (J = 23.75 Hz), and the IR stretches for the carbonyl ligands shift (powder sample, diamond ATR, cm^{-1}): ν_{12CO}: 2044, 1989; ν_{13CO}: 1999, 1946.

Stoichiometric Deoxygenative C−C Coupling

In a representative reaction, a solution of **4-^{13}CO** (30 mg, 0.027 mmol) in THF (1.5 mL) in a 20 mL scintillation vial charged with a stir bar was frozen in a liquid nitrogen-cooled cold well. A second solution of ^{i}Pr$_3$SiCl (20.8 mg, 0.108 mmol) in THF (0.5 mL) was likewise frozen. While thawing, the ^{i}Pr$_3$SiCl solution was added to the stirring deep purple solution of **4-^{13}CO**. As the reaction mixture continued to warm, the color changed to burgundy. An aliquot was removed and transferred to a J. Young NMR tube. C_6D_6 (100 µL) was added via Hamilton syringe. The aliquot was then analyzed by $^{13}C\{^1H\}$ and $^{31}P\{^1H\}$ NMR.

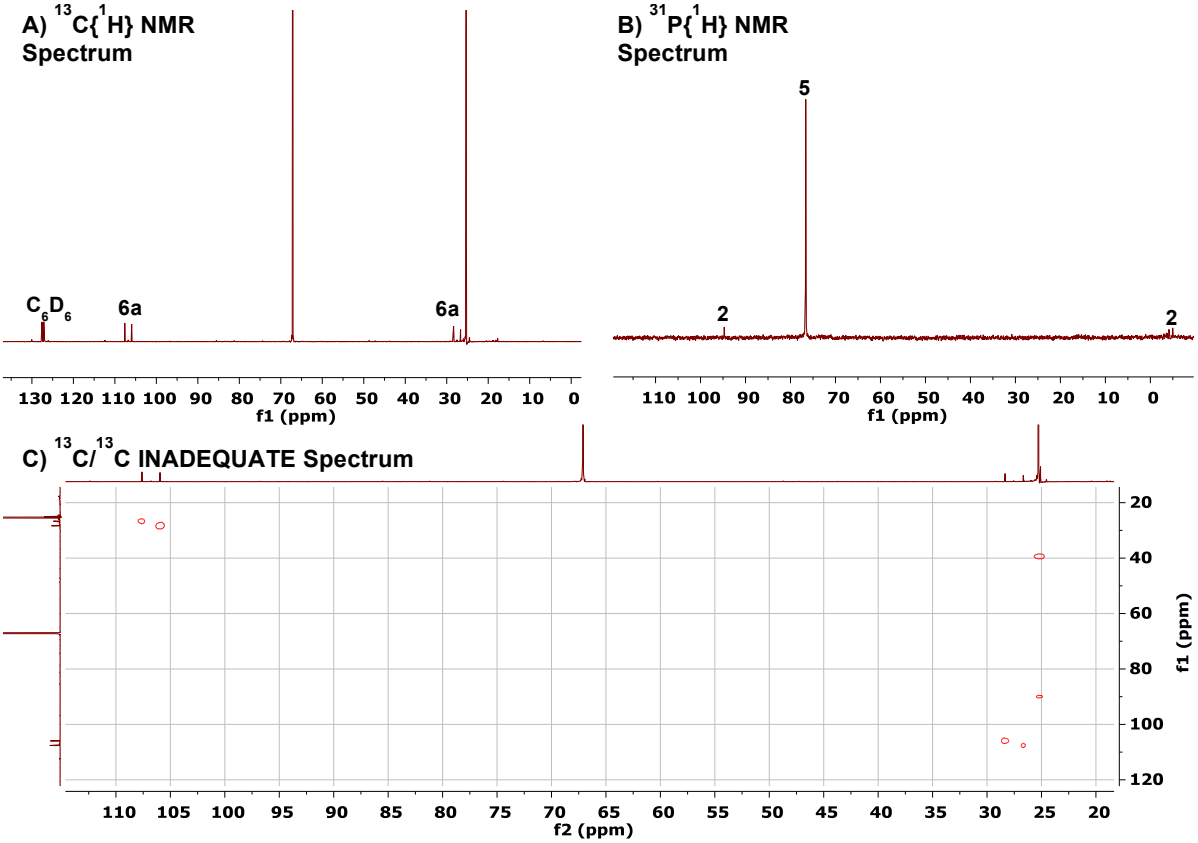

Figure S1—(A) $^{13}C\{^1H\}$ NMR spectrum (101 MHz, THF/C_6D_6, 25°C) showing the formation of **6a-^{13}CO**, following treatment of **4-^{13}CO** with excess ^{i}Pr$_3$SiCl. (B) The major metal containing product *ca.* 75% was identified as the dinitrogen complex **5**. (C) Strong C–C coupling ($^1J_{CC}$ = 167.74 Hz) consistent with **6a-^{13}CO** was verified via INADEQUATE NMR.

Hexamethyldisiloxane Detection

During a typical preparation of **7** (*vide supra*), following addition of Me_3SiCl to **3**, *ca.* 400 µL of the reaction mixture was transferred to a J. Young NMR tube. C_6D_6 (100 µL) was added via Hamilton syringe. The aliquot was then analyzed by $^{13}C\{^1H\}$ NMR (Figure S2, top). The J. Young tube was degassed via three freeze-pump-thaw cycles and an authentic sample of hexamethyldisiloxane was added via vacuum transfer. The contents of the tube were again analyzed by $^{13}C\{^1H\}$ NMR (Figure S2, bottom).

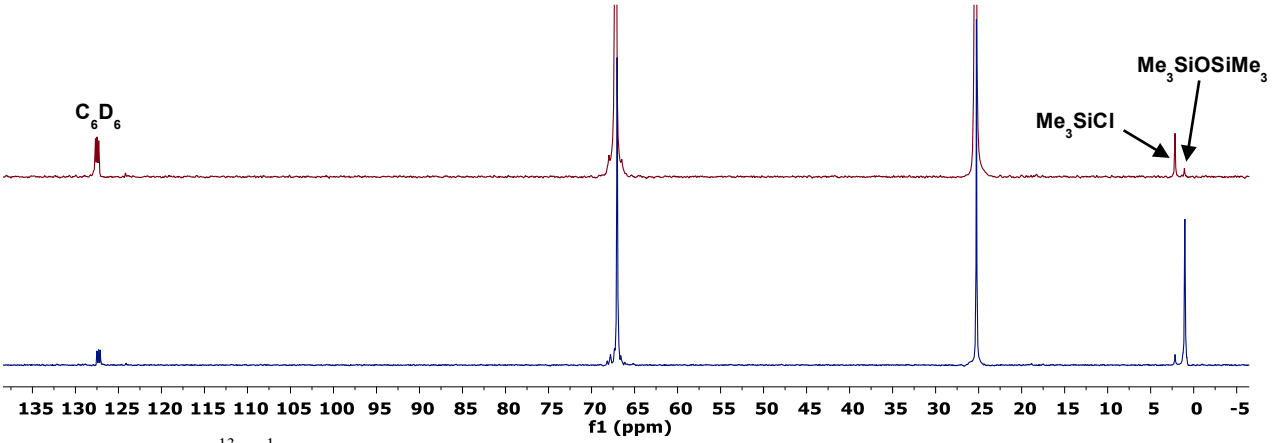

Figure S2—Partial $^{13}C\{^1H\}$ NMR spectrum (126 MHz, 25 °C, THF) of a representative reaction mixture following addition of excess Me_3SiCl to **3** before (top) and after (bottom) the addition of an authentic sample of $Me_3SiOSiMe_3$.

Silyl Alkylidyne Reduction

A 20 mL scintillation vial was charged with a stir bar, **7-^{13}CO** (20 mg, 0.028 mmol), and KC_8 (8 mg, 0.059 mmol). THF (1 mL) was added with stirring, resulting in the formation of a dark, heterogeneous mixture. The mixture was left to stir for 10 minutes, at which time it was filtered through a Celite plug into an NMR tube. $^{31}P\{^1H\}$ and $^{13}C\{^1H\}$ NMR spectroscopy demonstrated quantitative conversion of **7-^{13}CO** to **5** and silyl ethynolate **6b-^{13}CO** (Figure S3, B).[7] Addition of Me_3SiCl (2 drops) to this NMR tube led to the formation of **6c-^{13}CO** (major) and **6a^{Me}-^{13}CO** (minor) as evidenced by $^{13}C\{^1H\}$ NMR spectroscopy (Figure S3, C).[8,9]

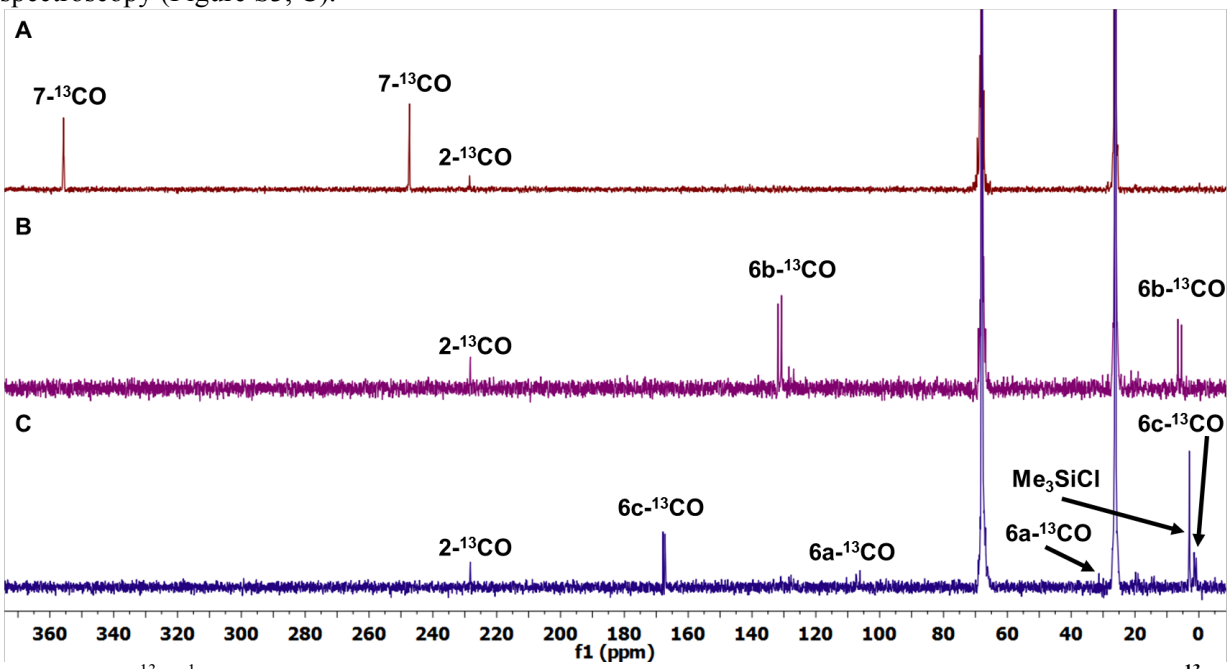

Figure S3—$^{13}C\{^1H\}$ NMR spectrum (126 MHz, 25 °C, THF) of the stepwise reduction and silylation of **7-^{13}CO**. $^{13}C\{^1H\}$ NMR spectroscopy (A) shows the characteristic resonances at 355.8 and 247.5 attributable to the silyl alkylidyne and carbonyl carbons of **7-^{13}CO**, respectively. Upon two electron reduction (B), formation of ethynolate **6b-^{13}CO** ($^{13}C\{^1H\}$ NMR (126 MHz, 25 °C, THF) δ = 131.34, 5.94, $^1J_{CC}$ = 139.6 Hz) is observed. Addition of Me_3SiCl to this mixture (C) yields ketene **6c-^{13}CO** ($^{13}C\{^1H\}$ NMR (126 MHz, 25 °C, THF) δ = 167.54, 1.13, $^1J_{CC}$ = 82.3 Hz). Minimal formation of **6a^{Me}-^{13}CO** is observed ($^{13}C\{^1H\}$ NMR (126 MHz, 25 °C, THF) δ = 106.7, 30.6, $^1J_{CC}$ = 163.7 Hz).

NMR Spectra

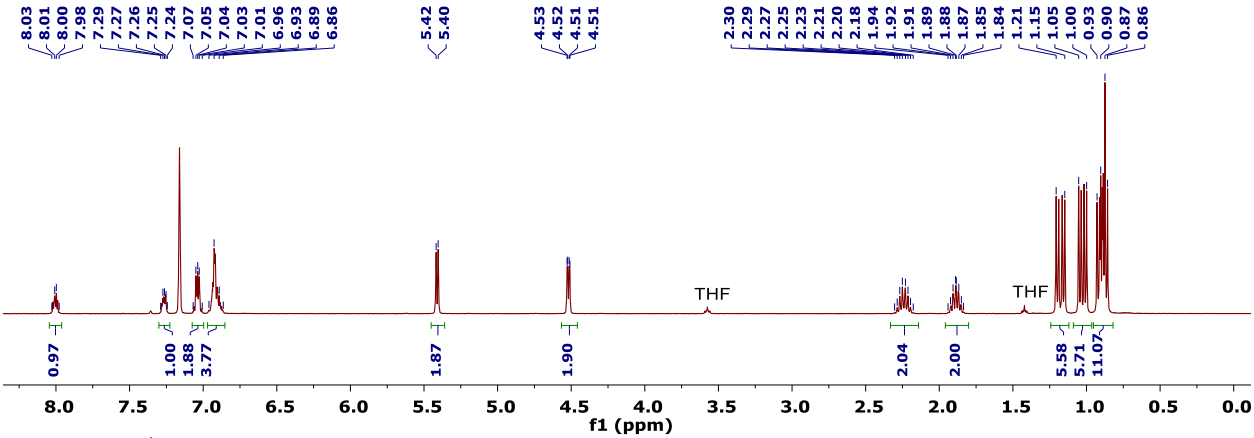

Figure S4—^{1}H NMR Spectrum (400 MHz, C_6D_6, 25°C) of **2**.

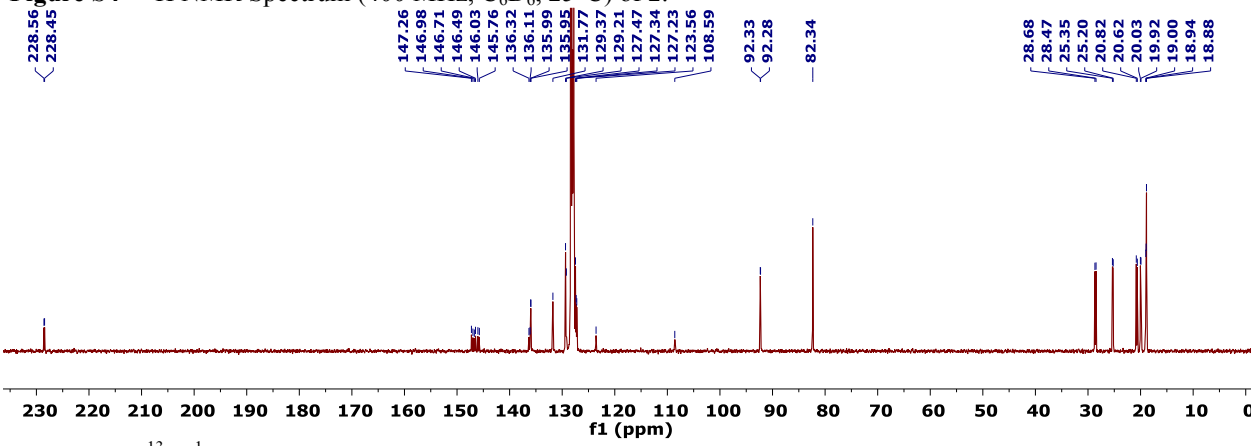

Figure S5—^{13}C{^{1}H} NMR Spectrum (101 MHz, C_6D_6, 25°C) of **2**.

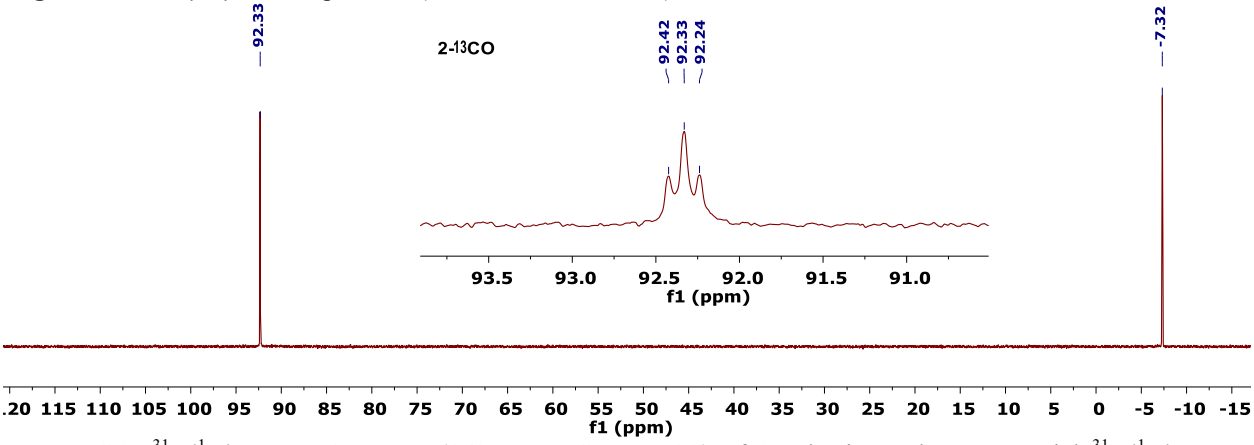

Figure S6—^{31}P{^{1}H} NMR Spectrum (162 MHz, C_6D_6, 25°C) of **2**. The inset shows a partial ^{31}P{^{1}H} NMR spectrum for **2-^{13}CO**.

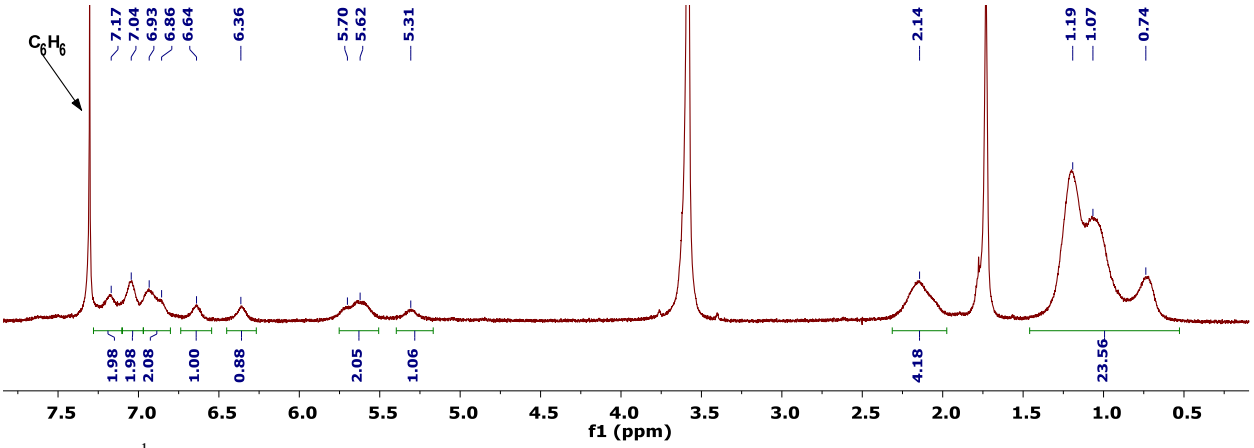

Figure S7—^{1}H NMR Spectrum (400 MHz, THF-d_8, 25°C) of **3**.

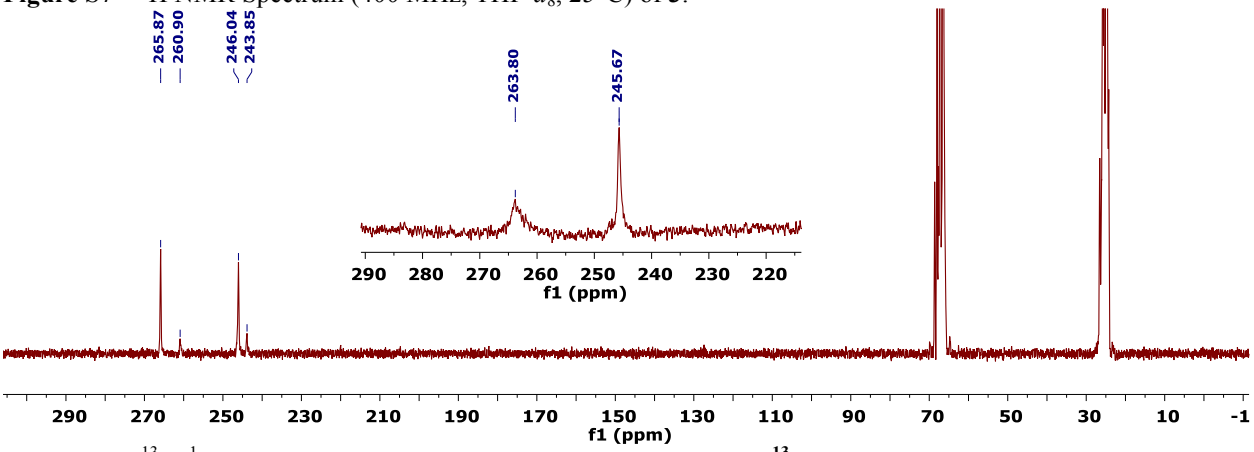

Figure S8—^{13}C{^{1}H} NMR Spectrum (126 MHz, THF-d_8, -80°C) of **3-^{13}CO**. The inset shows the downfield region of a ^{13}C{^{1}H} NMR spectrum of the same sample collected at 25 °C.

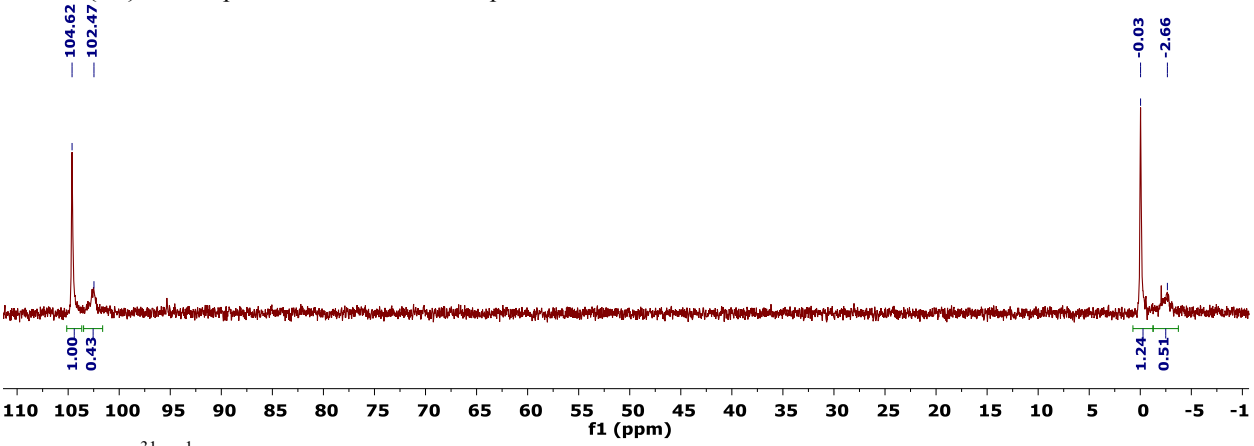

Figure S9—^{31}P{^{1}H} NMR Spectrum (162 MHz, THF-d_8, 25°C) of **3**.

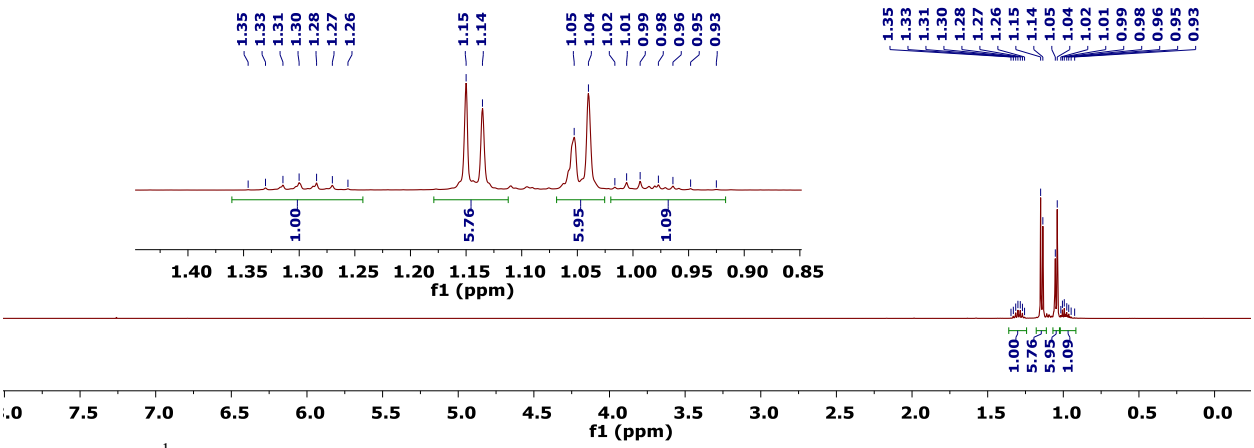

Figure S10—^{1}H NMR Spectrum (500 MHz, $CDCl_3$, 25°C) of **6a**. The inset contains and enlargement of the 0.85-1.45 ppm region.

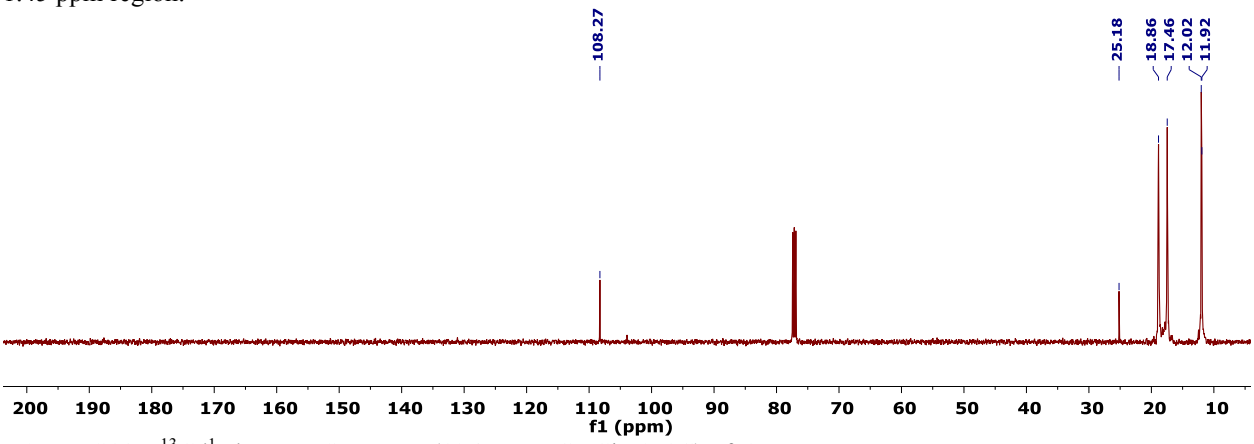

Figure S11—$^{13}C\{^{1}H\}$ NMR Spectrum (126 MHz, $CDCl_3$, 25°C) of **6a**.

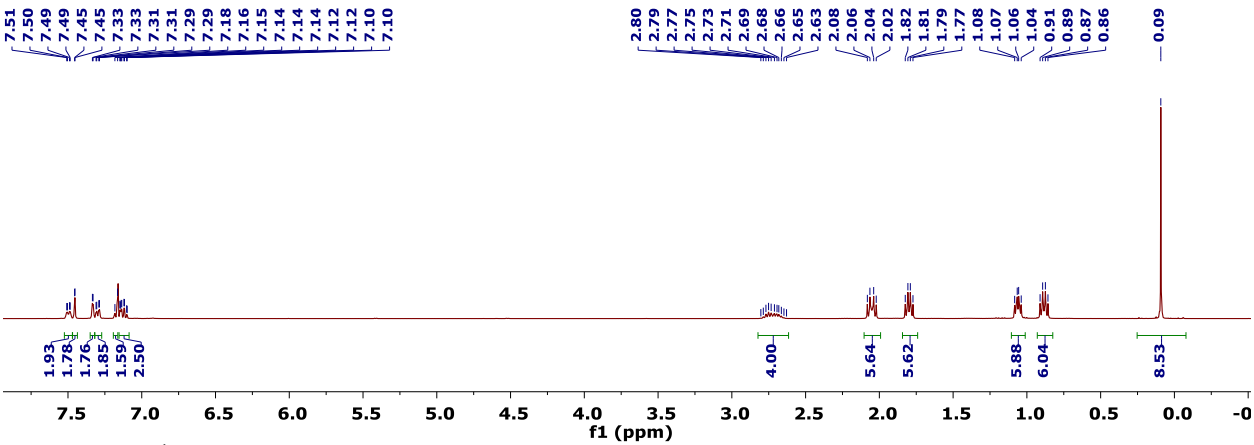

Figure S12—^{1}H NMR Spectrum (400 MHz, C_6D_6, 25°C) of **7**.

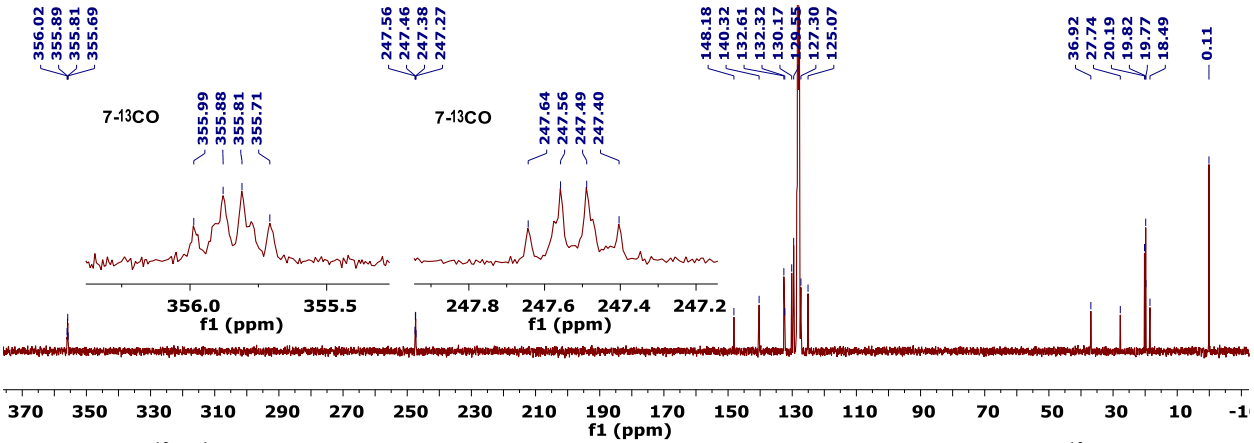

Figure S13—$^{13}C\{^{1}H\}$ NMR Spectrum (101 MHz, C_6D_6, 25°C) of **7.** The inset shows the enhanced ^{13}C signals for **7-^{13}CO**.

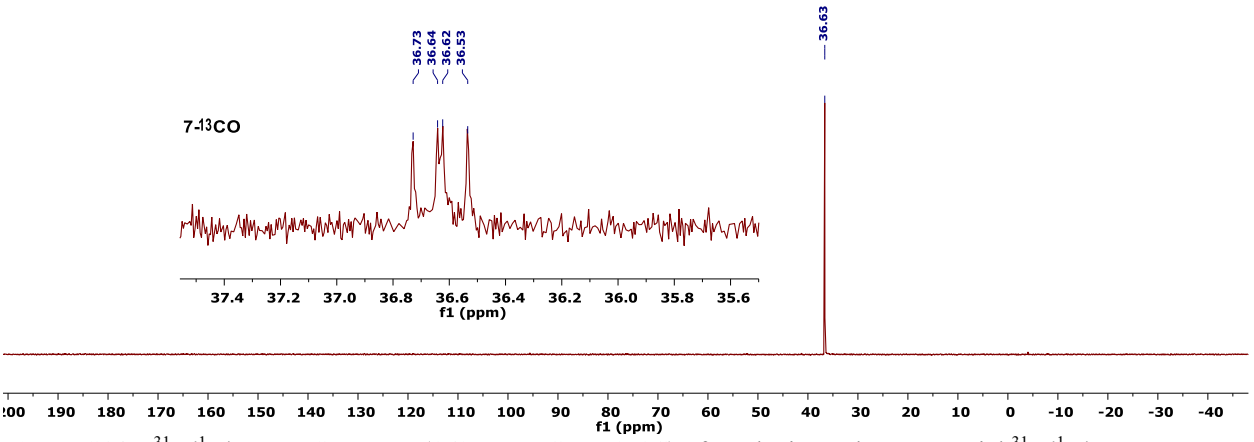

Figure S14—$^{31}P\{^{1}H\}$ NMR Spectrum (162 MHz, C_6D_6, 25°C) of **7**. The inset shows a partial $^{31}P\{^{1}H\}$ NMR spectrum for **7-^{13}CO**.

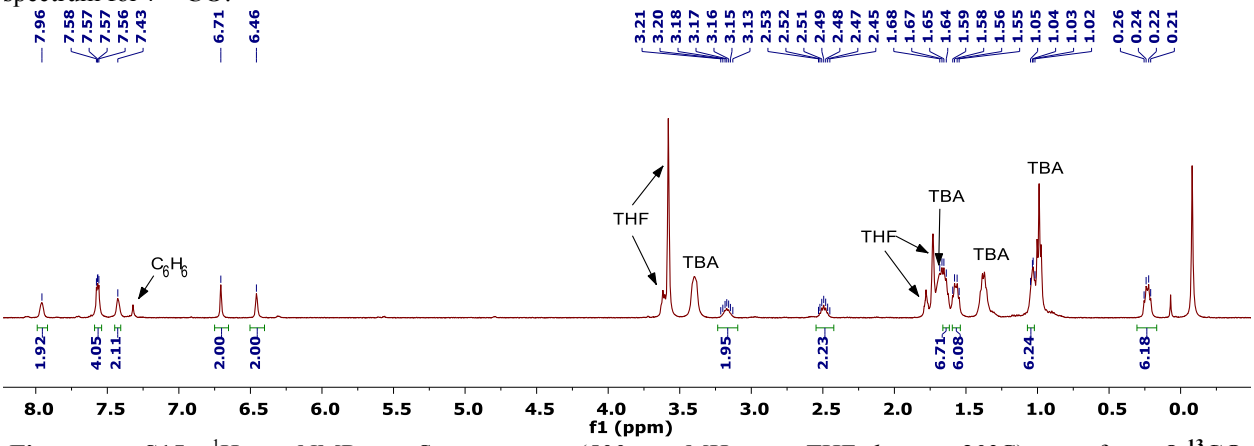

Figure S15—^{1}H NMR Spectrum (500 MHz, THF-d_8, -20°C) of **8-^{13}CO**.

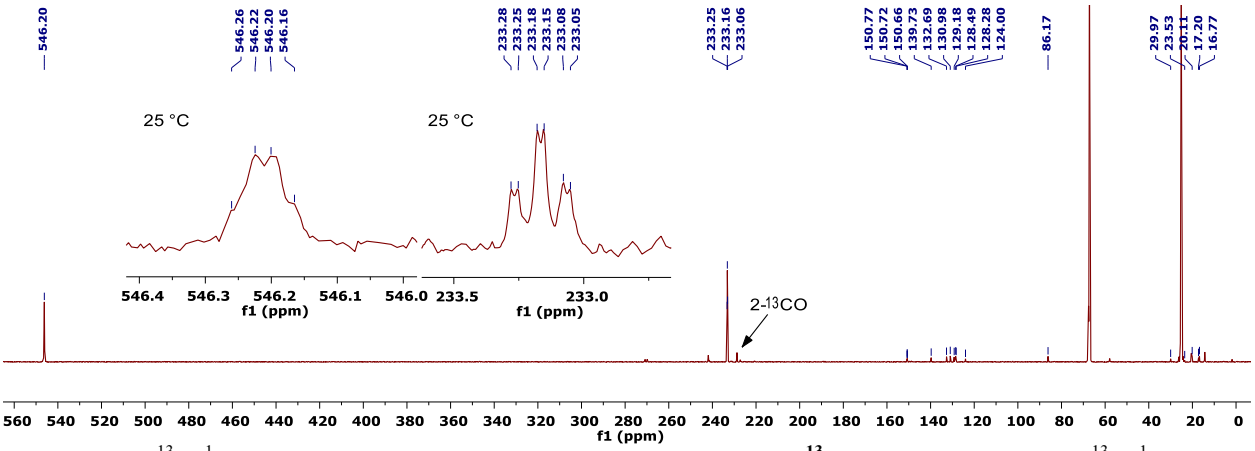

Figure S16—$^{13}C\{^{1}H\}$ NMR Spectrum (126 MHz, THF-d_8, -20°C) of **8-^{13}CO**. The inset shows a $^{13}C\{^{1}H\}$ NMR spectrum (126 MHz, THF/C_6D_6, 25 °C), demonstrating well resolved $^{2}J_{PC}$ and $^{2}J_{CC}$.

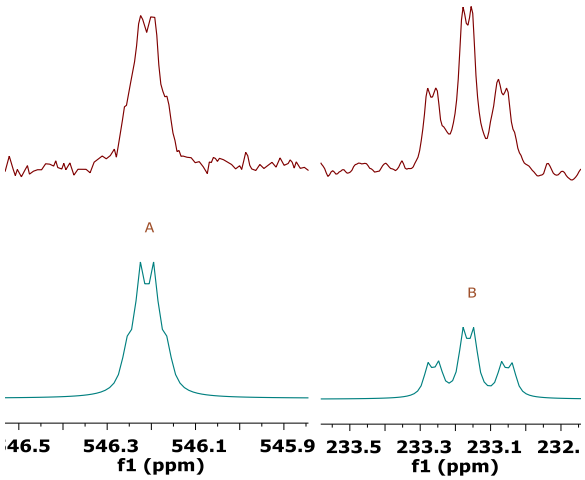

Figure S17—Partial $^{13}C\{^{1}H\}$ NMR Spectrum (126 MHz, THF/C_6D_6, 25 °C) of **8-^{13}CO** (top) and spin simulation thereof (bottom). The simulation matched the experimental data with the following coupling constants: $^{2}J_{CC}$ = 3.46 Hz, $^{2}J_{P(C:)}$ = 3.26 Hz, and $^{2}J_{P(CO)}$ = 12.55 Hz.

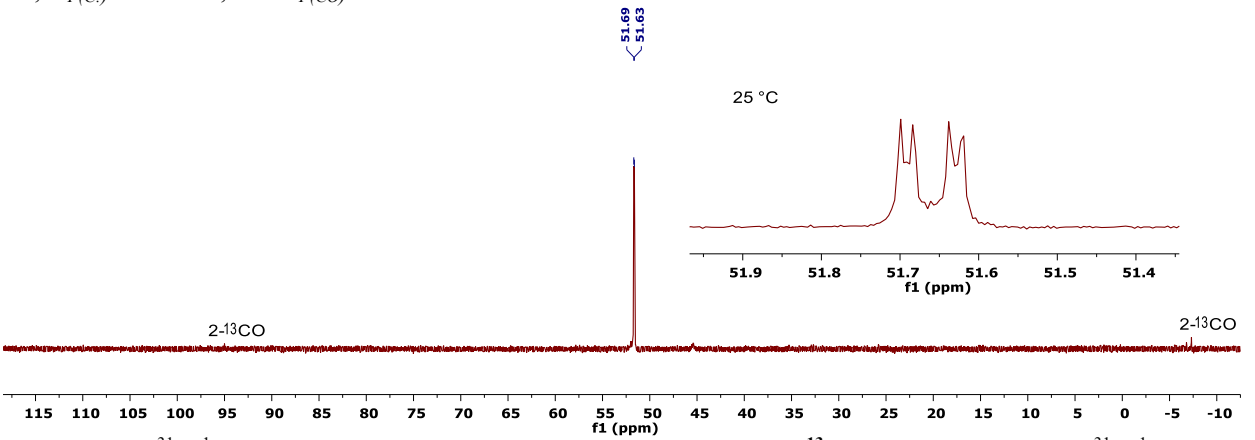

Figure S18—$^{31}P\{^{1}H\}$ NMR Spectrum (202 MHz, THF-d_8, -20°C) of **8-^{13}CO**. The inset shows a $^{31}P\{^{1}H\}$ NMR spectrum (202 MHz, THF/C_6D_6, 25 °C), demonstrating well resolved $^{2}J_{PC}$.

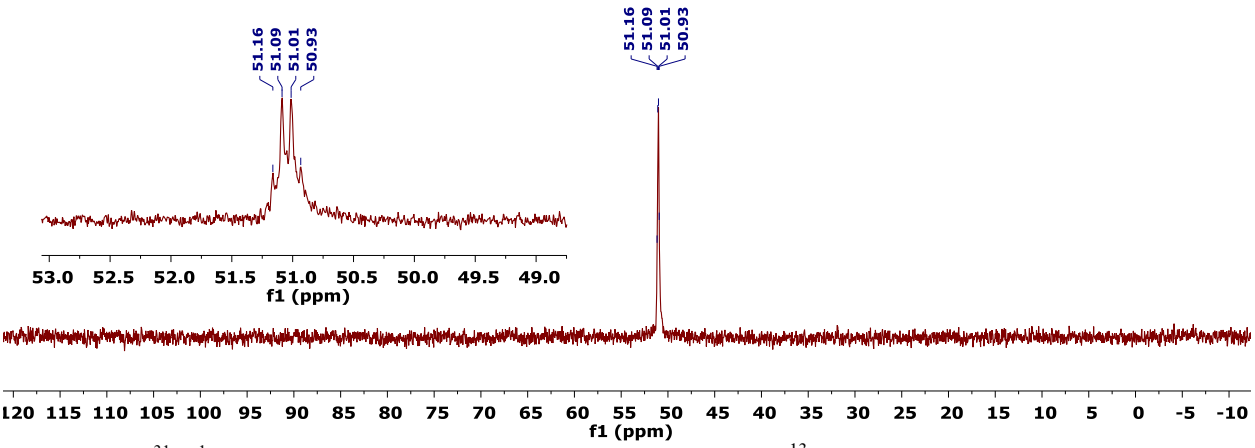

Figure S19—$^{31}P\{^{1}H\}$ NMR Spectrum (300 MHz, C_6D_6, 25°C) of $P_2Mo(^{13}CO)_3$. The inset contains an enlargement of the quartet at 51.05 ppm.

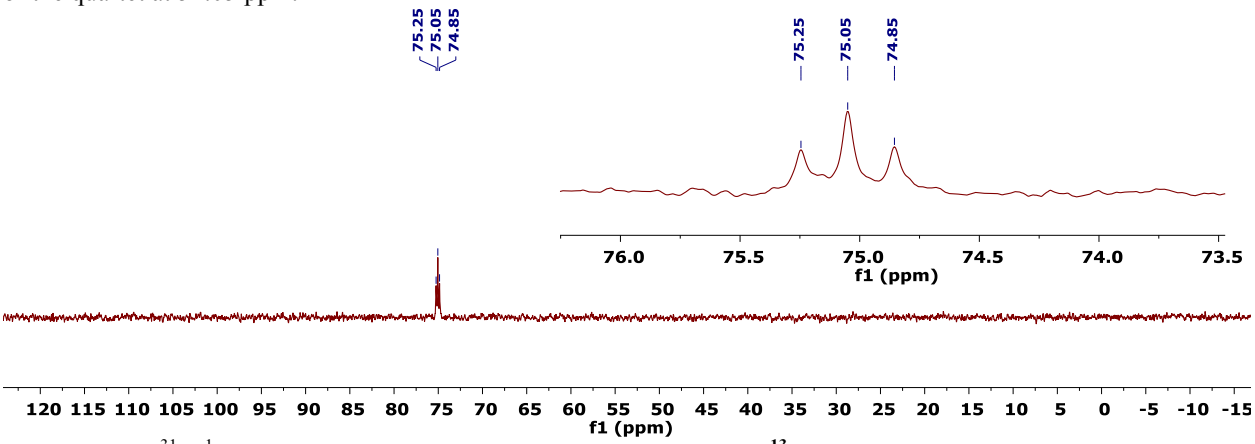

Figure S20—$^{31}P\{^{1}H\}$ NMR Spectrum (300 MHz, CD_3CN, 25°C) of **1-^{13}CO**. The inset contains and enlargement of the triplet at 75.05 ppm.

IR Spectra

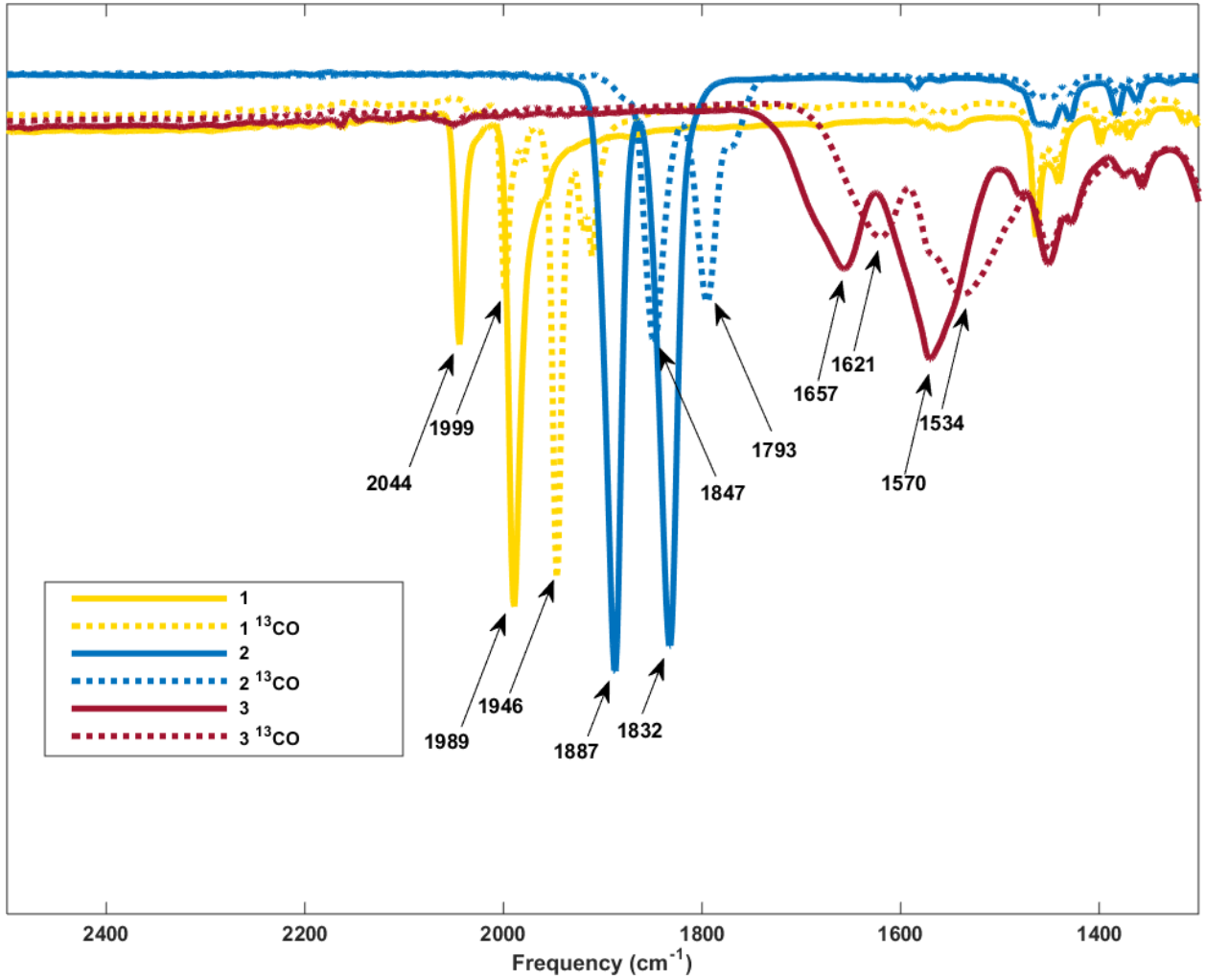

Figure S21—ATR IR Spectra of **1**, **1-^{13}CO**, **2**, **2-^{13}CO**, **3**, and **3-^{13}CO**, showing increased Mo–CO backbonding upon sequential reduction. The difference in the stretching frequency of the ^{12}C and ^{13}C isotopologs matches well with values calculated using a simple oscillator model and the respective reduced masses.

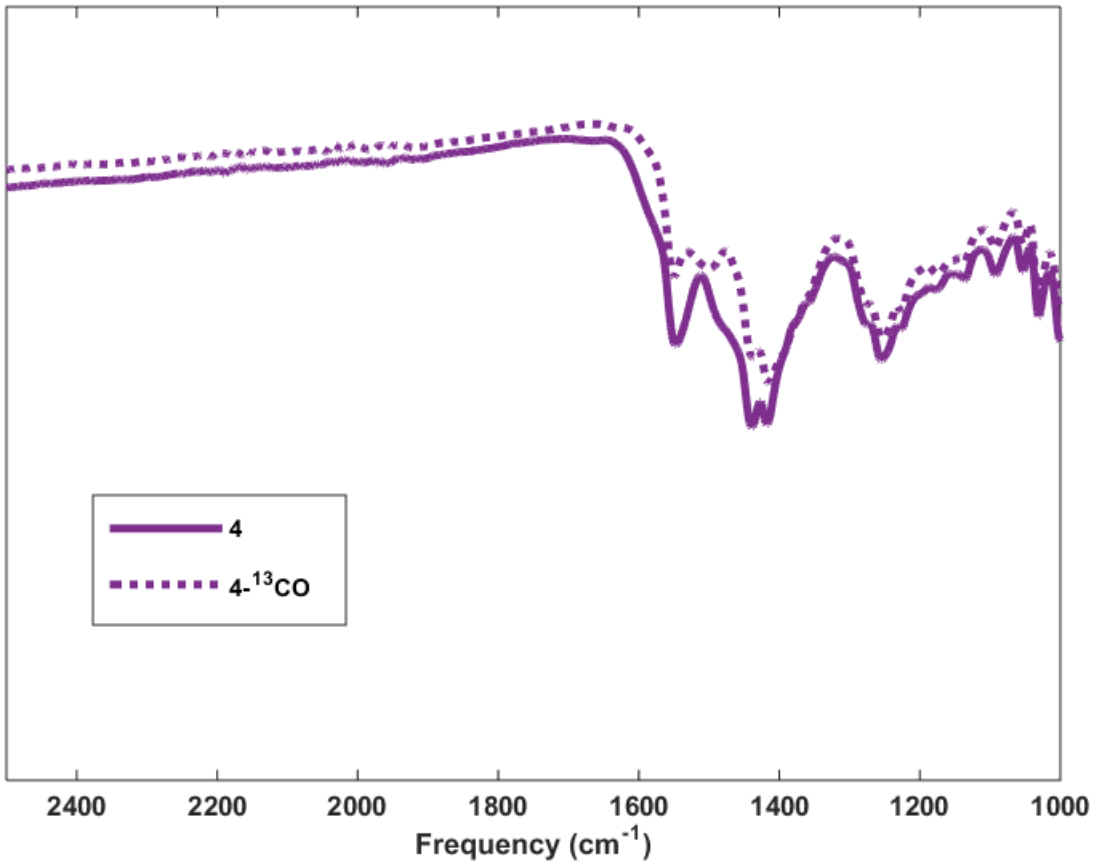

Figure S22—ATR IR Spectra of **4** and **4-^{13}CO**. The weakened, low-frequency bands for the CO stretches cannot be differentiated from ligand resonances in the fingerprint region, despite isotopic labelling.

Crystallographic Information

CCDC deposition numbers 1412062-1412064 and 1412068 contain the supplementary crystallographic data for this paper. These data can be obtained free of charge from The Cambridge Crystallographic Data Centre via www.ccdc.cam.ac.uk/data_request/cif.

Refinement Details—In each case, crystals were mounted on a glass fiber or MiTeGen loop using Paratone oil, then placed on the diffractometer under a nitrogen stream. Crystals for compounds **3** and **4** were manipulated under an Argon purge due to atmospheric sensitivity. Low temperature (100 K) X-ray data were obtained on a Bruker KAPPA APEXII CCD based diffractometer (Mo fine-focus sealed X-ray tube, K_α = 0.71073 Å) or a Bruker D8 VENTURE Kappa Duo PHOTON 100 CMOS based diffractometer (Mo $I_\mu S$ HB micro-focus sealed X-ray tube, K_α = 0.71073 Å OR Cu $I_\mu S$ HB micro-focused X-ray tube, K_α = 1.54178). All diffractometer manipulations, including data collection, integration, and scaling were carried out using the Bruker APEXII software.[10] Absorption corrections were applied using SADABS.[11] Space groups were determined on the basis of systematic absences and intensity statistics and the structures were solved in the Olex 2 software interface[12] by intrinsic phasing using XT (incorporated into SHELXTL)[13] and refined by full-matrix least squares on F^2. All non-hydrogen atoms were refined using anisotropic displacement parameters. Hydrogen atoms were placed in the idealized positions and refined using a riding model. The structure was refined (weighed least squares refinement on F^2) to convergence. Graphical representation of structures with 50% probability thermal ellipsoids were generated using Diamond 3 visualization software.[14]

Table S1—Crystal and refinement data for complexes **2-4** and **7**.

	2	**3**	**4**	**7**
CCDC Number[15]	1412068	1412062	1412063	1412064
Empirical formula	$C_{38}H_{46}MoO_2P_2$	$C_{96}H_{144}K_4Mo_2O_{12}P_4$	$C_{178}H_{264}K_{12}Mo_4O_{18}P_8$	$C_{35}H_{49}ClMoOP_2Si$
Formula weight	692.63	1962.26	3792.60	707.16
T (K)	100	100	100	100
a, Å	17.1790(7)	13.2319(5)	24.1145(8)	9.1531(2)
b, Å	7.4663(3)	15.1410(6)	21.1590(7)	17.1136(4)
c, Å	27.0465(12)	25.4501(10)	38.2636(12)	21.8842(6)
α, °	90	101.2840(10)	90	90
β, °	91.405(2)	100.0870(10)	94.002(2)	90
γ, °	90	90.0560(10)	90	90
Volume, Å^3	3468.0(3)	4919.6(3)	19476.0(11)	3428.00(14)
Z	4	2	4	4
Crystal system	Monoclinic	Triclinic	Monoclinic	Orthorhombic
Space group	$P2_1/n$	$P\bar{1}$	$P2_1/c$	$P2_12_12_1$
d_{calc}, g/cm^3	1.327	1.325	1.293	1.370
θ range, °	1.389 to 45.898	2.203 to 37.810	2.315 to 75.840	2.209 to 37.904
μ, mm^{-1}	0.502	0.546	5.420	0.615
Abs. Correction	Semi-empirical	Semi-empirical	Semi-empirical	Semi-empirical
GOF	1.032	1.080	1.012	1.086
R_1,[a] wR_2[b] [I>2 σ(I)]	0.0286, 0.0653	0.0748, 0.1285	0.0644, 0.1463	0.0395, 0.0742
Diffractometer	APEXII	PHOTON	PHOTON	PHOTON
Radiation Type	Mo K_α	Mo K_α	Cu K_α	Mo K_α

[a] $R_1 = \sum||F_o| - |F_c||/\sum|F_o|$. [b] $wR_2 = [\sum[w(F_o^2-F_c^2)^2]/\sum[w(F_o^2)^2]]^{1/2}$.

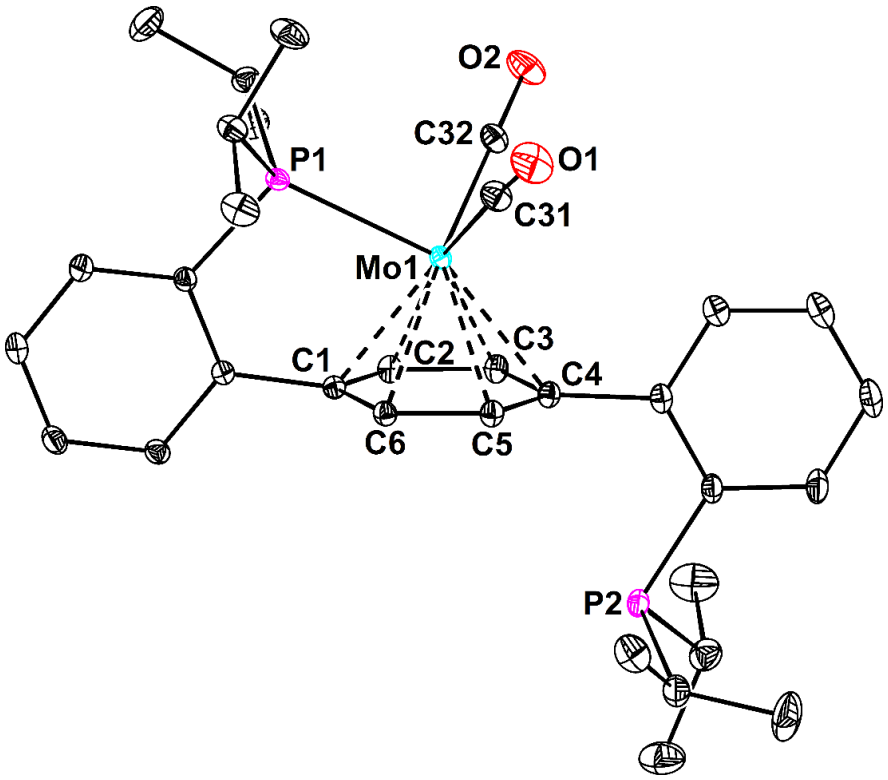

Figure S23—Structural drawing of **2** with 50% probability anisotropic displacement ellipsoids. Co-crystallized benzene and hydrogen atoms are omitted for clarity.

Special Refinement Details for 2—The co-crystallized benzene molecule was disordered over two positions and satisfactorilly modeled in a 67:33 ratio. 1,2 and 1,3 distances of the minor component were restrained to be equivalent to those of the major component. Automatic bond generation was suppresed between the disordered groups.

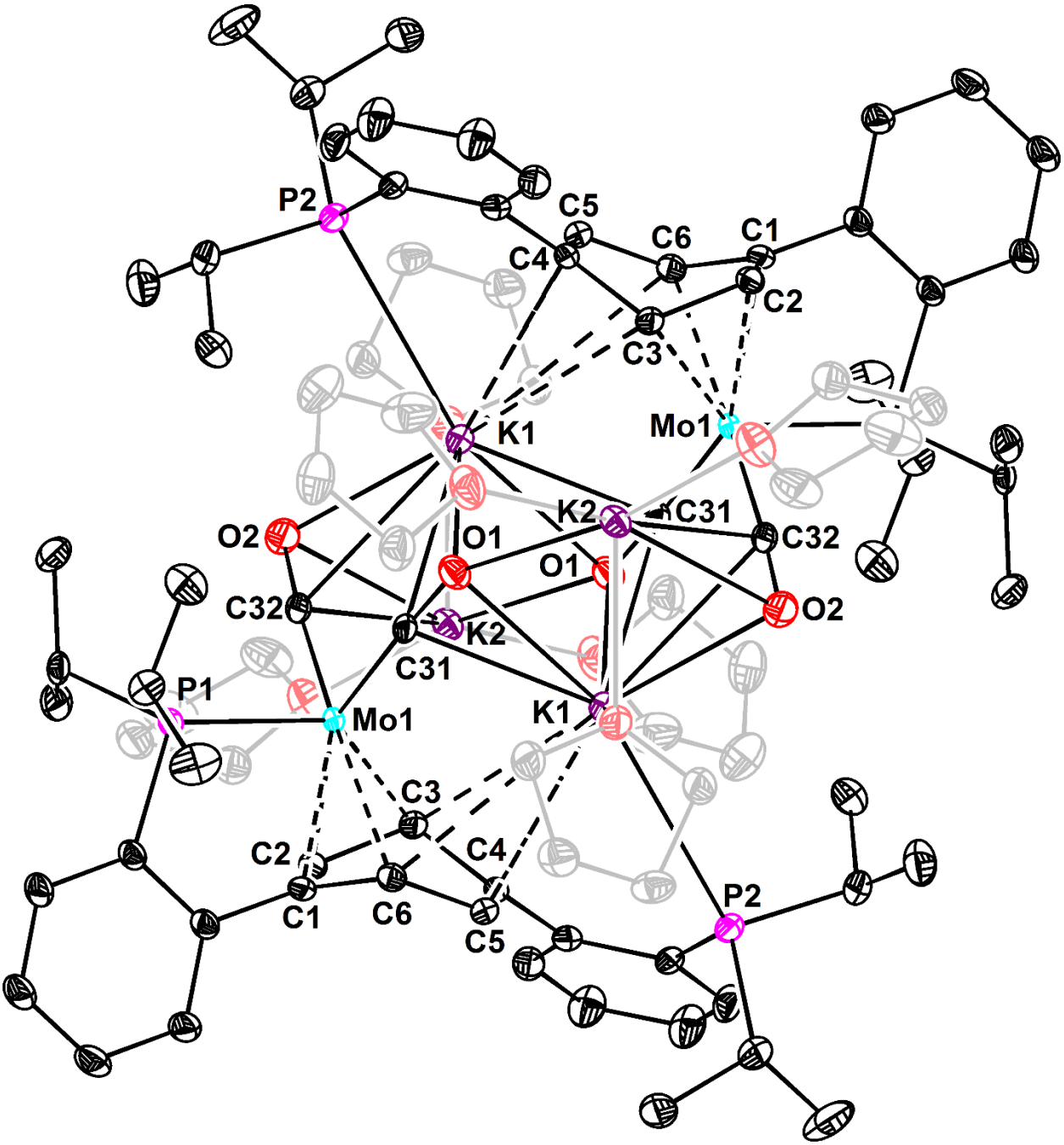

Figure S24—Structural drawing of **3** with 50% probability anisotropic displacement ellipsoids. K-bound THF molecules are represented in grey. Co-crystallized THF molecules and hydrogen atoms are omitted for clarity.

Special Refinement Details for 3—One of the ligand isopropyl groups, three of the K-bound THF molecules, and one of the co-crystallized THF molecules were positionally disordered. In each case, the disorder was modeled satisfactorily with populations as follow: C60 through C62 58%, C1A through C1C 42%; C78A 47%, C78B 53%; O9A and C82A through C84A 28%, O9B and C82B through C84B 72%; O10A and C86A 20%, O10B and C86B 80%; and O12A through C96A 33%, O12B through C96B 67%. Automatic bond generation was suppressed between disordered groups.

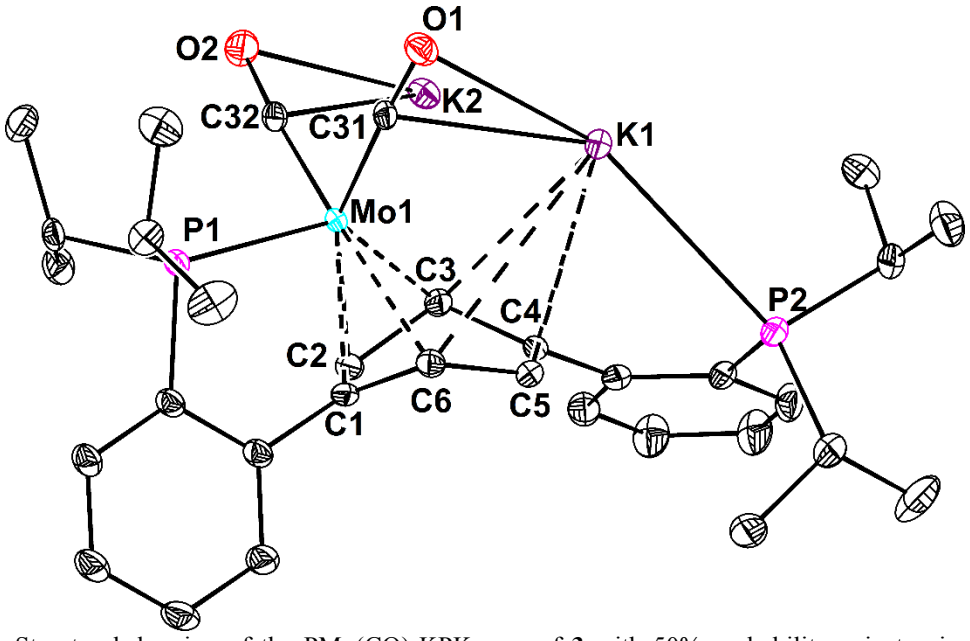

Figure S25—Structural drawing of the $PMo(CO)_2KPK$ core of **3** with 50% probability anisotropic displacement ellipsoids. Co-crystallized THF molecules, K-bound THF molecules, and hydrogen atoms are omitted for clarity.

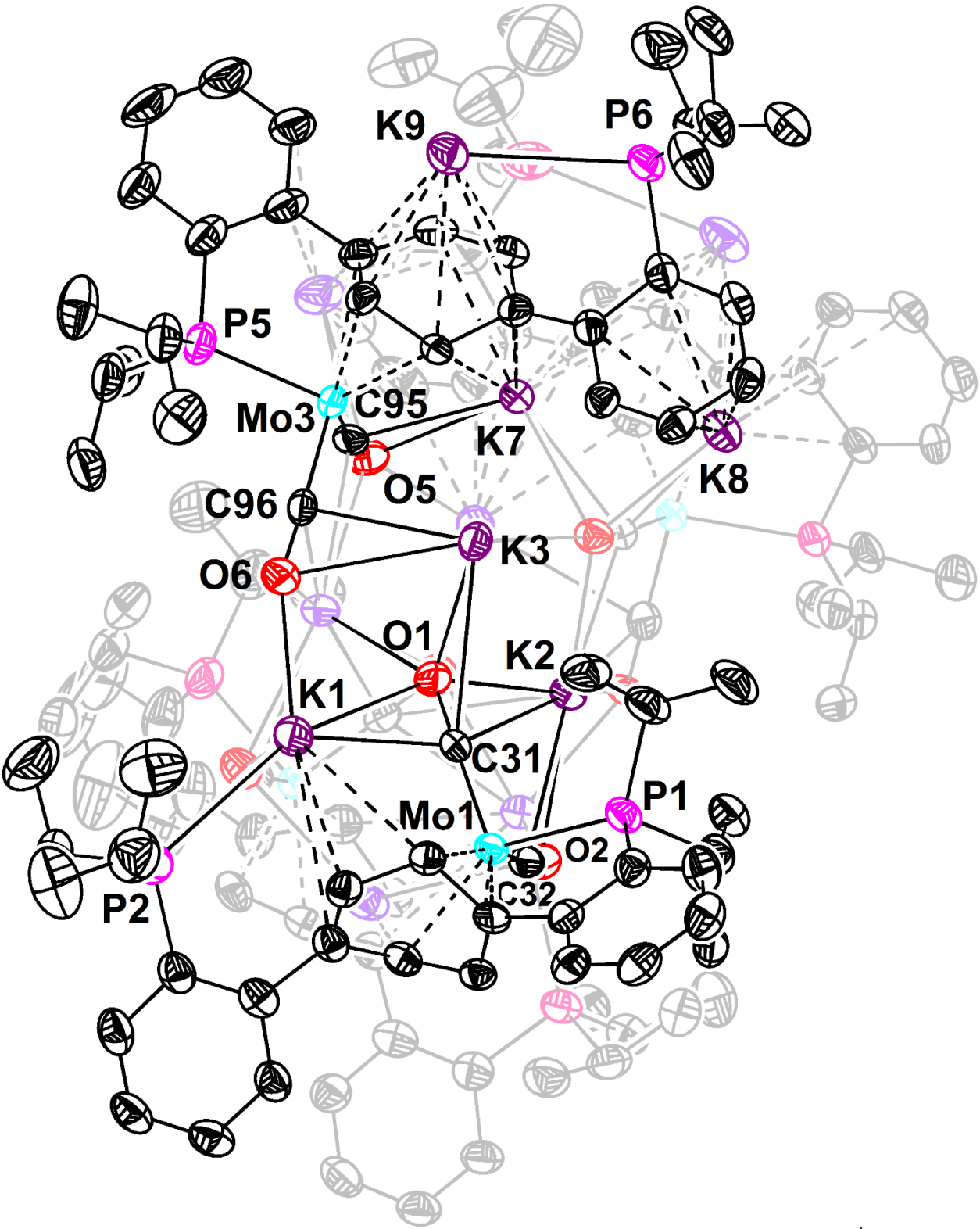

Figure S26—Structural drawing of **4** with 50% probability anisotropic displacement ellipsoids. The η^4 (bottom) and η^3 (top) subunits located in the back of the tetramer are represented in grey. K-bound THF molecules, co-crystallized pentane molecules, and hydrogen atoms are omitted for clarity.

Special Refinement Details for 4—There was significant positional disorder in all but two of the K-bound THF molecules in the structure. The disordered groups were satisfactorily modeled over two to four positions with populations as follows: O11 through C161 30%, O11A through C261 17%, O11B through C361 27%, O11C through C461 26%; O12 through C165 34%, O12A through C265 66%; O13 through C169 59%, O13A through C269 41%; O14 through C173 39%, O14A through C273 26%, O14B through C373 35%; O15 through C177 69%, O15A through C277 31%; O16 through C181 62%, O16A through C281 38%; O17 through C185 53%, O17A through C285 47%; and O18 through C189 52%, O18A through C289 48%. The 1,2 and 1,3 distances of these disordered THF groups were restrained to be equivalent to those of one of the single-site K-bound THF molecules (O9 through C153). In the case of the most heavily disordered THF molecule (O14 through C173, O14A through C273, O14B through C373), the K–O distances were restrained to be similar to those of a single-site THF molecule (O9 through C153). One of the co-crystallized pentane molecules was also disordered over two sites, complementary to one of the K-bound THF molecules (O17 through C185, O17A through C285). Both components were satisfactorily modeled, tied to the population of the corresponding THF fragment, and restrained to have 1,2 and 1,3 distances equivalent to the undisordered pentane solvate. Further, all disordered moieties were refined with similarity restraints on U_{ij} and rigid bond restraints. Automatic bond generation was suppressed between disordered groups. One of the ligand isopropyl groups and one of the co-crystallized pentane molecules were disordered, but could not be satisfactorily modeled over two sites, even with restraints. Since the residual density for these groups was minor (*ca.* 8% of a carbon atom), they were left as single components.

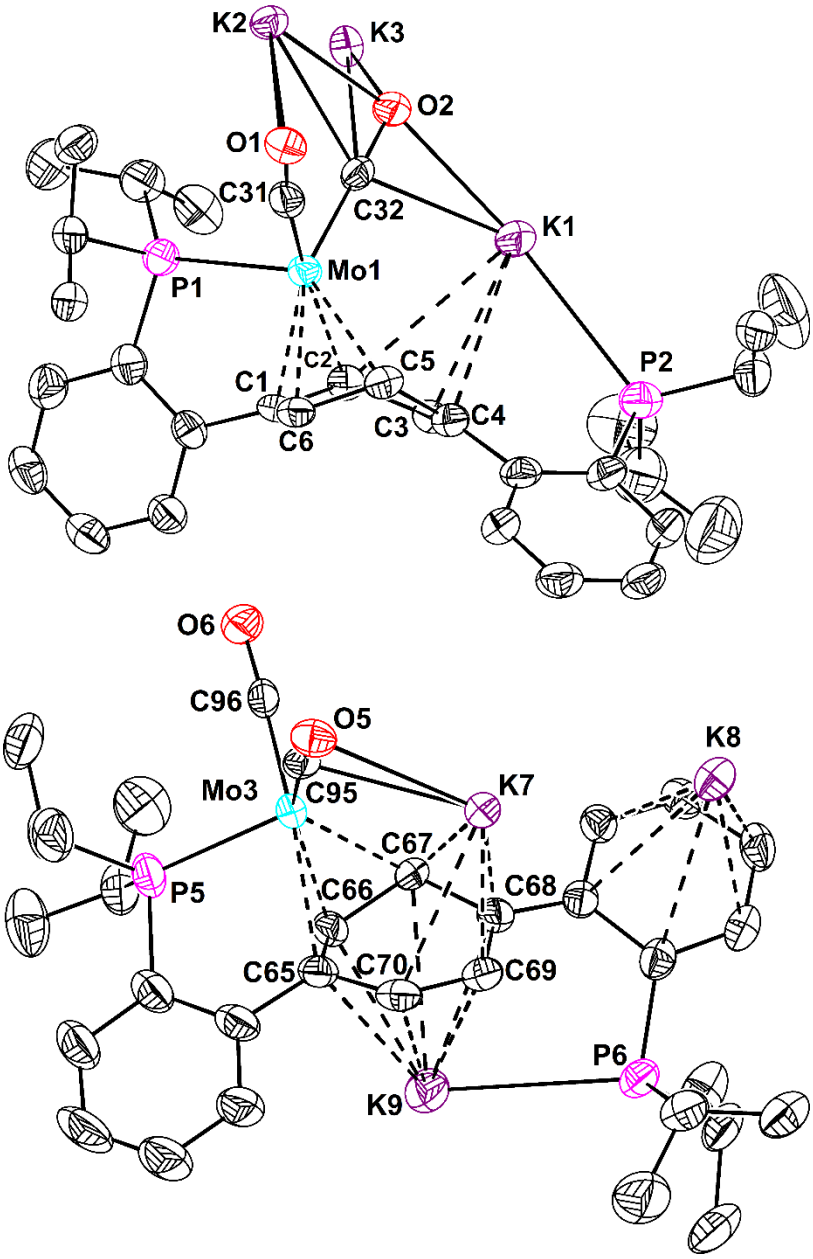

Figure S27—Structural drawing of the two distinct $PMo(CO)_2KPK_2$ cores of **4** with 50% probability anisotropic displacement ellipsoids. Co-crystallized THF and hydrogen atoms are omitted for clarity.

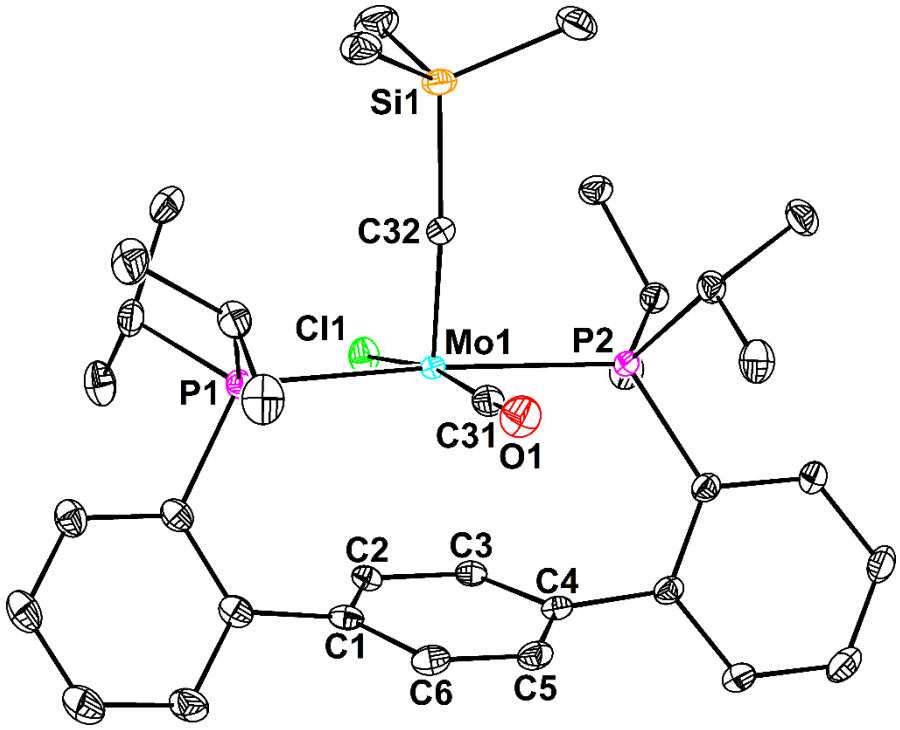

Figure S28—Structural drawing of **7** with 50% probability anisotropic displacement ellipsoids. Hydrogen atoms are omitted for clarity.

Table S2—Selected structural data for complexes **2-4,** and **7.**

	2	**3**	**4 (η^4)**	**4 (η^3)**	**7**
Mo–P1	2.4191(2)	2.4063(6)	2.401(2)	2.402(1)	2.5869(6)
Mo–P2	N/A	N/A	N/A	N/A	2.5562(6)
Mo–C_{arene} (ave.)	2.3254(6)	2.344(2)	2.336(6)	2.319(5)	2.82 (contact)
Mo–C31	1.9675(7)	1.921(2)	1.916(7)	1.902(6)	1.974(2)
Mo–C32	1.9710(6)	1.908(2)	1.889(6)	1.910(7)	1.767(2)
C1–C2	1.4183(8)	1.395(3)	1.449(9)	1.473(8)	1.395(3)
C2–C3	1.4216(8)	1.481(3)	1.463(8)	1.482(7)	1.392(3)
C3–C4	1.4210(8)	1.507(3)	1.360(8)	1.502(7)	1.401(3)
C4–C5	1.4214(8)	1.356(3)	1.490(8)	1.427(7)	1.390(3)
C5–C6	1.4254(8)	1.464(3)	1.491(8)	1.373(8)	1.393(3)
C6–C1	1.4272(8)	1.455(3)	1.381(9)	1.448(8)	1.395(3)
C31–O1	1.1632(9)	1.200(3)	1.225(7)	1.252(7)	1.138(3)
C32–O2	1.1645(8)	1.219(3)	1.227(7)	1.226(7)	N/A
C32–Si1	N/A	N/A	N/A	N/A	1.877(2)
O1–Si1	N/A	N/A	N/A	N/A	N/A
O2–Si2	N/A	N/A	N/A	N/A	N/A
∠C31-Mo1-C32	85.01(3)	89.1(1)	87.7(2)	92.6(2)	87.4(1)

References

1. Pangborn, A. B., Giardello, M. A., Grubbs, R. H., Rosen, R. K. & Timmers, F. J. Safe and Convenient Procedure for Solvent Purification. *Organometallics* **15**, 1518-1520, (1996)
2. Buss, J. A., Edouard, G. A., Cheng, C., Shi, J. & Agapie, T. Molybdenum Catalyzed Ammonia Borane Dehydrogenation: Oxidation State Specific Mechanisms. *J. Am. Chem. Soc.* **136**, 11272-11275, (2014)
3. Weitz, I. S. & Rabinovitz, M. The Application of C_8K for Organic Synthesis: Reduction of Substituted Naphthalenes. *J. Chem. Soc., Perkin Trans. 1*, 117-120, (1993)
4. Danheiser, R. L., Nishida, A., Savariar, S. & Trova, M. P. Trialkylsilyloxyalkynes: Synthesis and Aromatic Annulation Reactions. *Tetrahedron Lett.* **29**, 4917-4920, (1988)
5. Sun, H. & DiMagno, S. G. Anhydrous Tetrabutylammonium Fluoride. *J. Am. Chem. Soc*. **127**, 2050-2051, (2005)
6. Fulmer, G. R. *et al.* NMR Chemical Shifts of Trace Impurities: Common Laboratory Solvents, Organics, and Gases in Deuterated Solvents Relevant to the Organometallic Chemist. *Organometallics* **29**, 2176-2179, (2010)
7. Ito, M., Shirakawa, E. & Takaya, H. Generation of Silylethynolates via C–Si Bond Cleavage of Disilylketenes Induced by t-BuOK. *Synlett*, 1329-1331, (2002)
8. Groh, B. L., Magrum, G. R. & Barton, T. J. Direct Conversion of 2,3-dihydrofurans to Silylsiloxyalkynes and Bis(silyl)ketenes. *J. Am. Chem. Soc.* **109**, 7568-7569, (1987)
9. Nikolaeva, S. N., Ponomarev, S. V., Petrosyan, V. S. & Lorberth, J. Silylation of Silylketenes. *J. Organomet. Chem.* **535**, 213-215, (1997)
10. APEX2, Version 2 User Manual, M86-E01078, Bruker Analytical X-ray Systems, Madison, WI, June 2006.
11. Sheldrick, G.M. "SADABS (version 2008/1): Program for Absorption Correction for Data from Area Detector Frames", University of Göttingen, 2008.
12 Dolomanov, O. V., Bourhis, L. J., Gildea, R. J., Howard, J. A. K. & Puschmann, H. OLEX2: A Complete Structure Solution, Refinement and Analysis Program. *J. Appl. Cryst.* **42**, 339-341, (2009)
13. Sheldrick, G.M. A Short History of SHELX. *Acta. Cryst.* **A64**, 112-122 (2008)
14. Brandenburg, K. (1999). DIAMOND. Crystal Impact GbR, Bonn, Germany.
15 Crystallographic data have been deposited at the CCDC, 12 Union Road, Cambridge CB2 1EZ, UK and copies can be otained on request, free of charge, by quoting the publication citation and the respective deposition numbers.